The source, fate, and transport of arsenic in the Yellowstone hydrothermal system - an overview

R. Blaine McCleskey[a*], D. Kirk Nordstrom[a], Shaul Hurwitz[b], Daniel R. Colman[c], David A. Roth[a], Madeline Johnson[a], and Eric S. Boyd[c]

[a] *U.S. Geological Survey, 3215 Marine St., Boulder, CO, 80303 USA*

[b] *U.S. Geological Survey, California Volcano Observatory, Moffett Field, CA 94035 USA*

[c] *Department of Microbiology and Cell Biology, Montana State University, Bozeman, MT 59717*

*Corresponding author: E-mail: rbmccles@usgs.gov

Conflict of interest: The authors declare that they have no competing interests.

Keywords:

Arsenic, Yellowstone, hydrothermal, microbial transformation, aqueous geochemistry, hot spring

Abstract

The Yellowstone Plateau Volcanic Field (YPVF) contains more than 10,000 thermal features including hot springs, pools, geysers, mud pots, and fumaroles with diverse chemical compositions. Arsenic (As) concentrations in YPVF thermal waters typically range from 0.005 to 4 mg/L, but an As concentration of 17 mg/L has been reported. Arsenic data from thermal springs, outflow drainages, rivers, and from volcanic rocks and silica sinter were used to identify the sources, characterize geochemical and microbial processes affecting As, and quantify As fluvial transport. Arsenic in YPVF thermal waters is mainly derived from high temperature leaching of rhyolites. Arsenic concentrations in thermal waters primarily depend on water type, which is controlled by boiling, evaporation, mixing, and mineral precipitation and dissolution. Springs with low As concentrations include acid-SO_4 (0.1 ± 0.1 mg/L), NH_4-SO_4 rich (0.003 ± 0.007 mg/L), and dilute thermal waters (0.1 ± 0.1 mg/L); travertine-forming waters have moderate As concentrations (0.4 ± 0.2 mg/L); and neutral- Cl waters (1.2 ± 0.8 mg/L) common in the western portion of the Yellowstone Caldera and Cl-rich waters (1.9 ± 1.2 mg/L) primarily from Basins near the Caldera boundary have elevated As concentrations. Reduced As species (arsenite and thiolated-As species) are most prevalent near the orifice of hot springs, and then As rapidly oxidizes to arsenate along drainages. Previously published cultivation-based studies and metagenomic data from microbial communities inhabiting a variety of hot springs indicate a widespread distribution of arsenite oxidation and arsenate reduction capabilities among the hot springs. Widespread use and transformation of As by thermophilic microorganisms promotes more soluble and toxic forms. Most of the water discharged from thermal springs eventually ends up in a nearby river where As remains soluble and exhibits little attenuation during downstream transport. Since 2010, 183 ± 10 metric tons/year of As were transported from

Yellowstone National Park (YNP) via rivers. The discharge from YPVF thermal features impairs river water quality whereby As concentrations exceed 10 µg/L for many rivers reaches within and downstream from YNP.

1. Introduction

Arsenic (As) is a geogenic contaminant in surface and groundwaters that is a considerable public-health concern (Bowell et al., 2014; World Health Organization, 2006). Since As is a known carcinogen, the United States Environmental Protection Agency (EPA) set the As standard for drinking water at 10 ppb (or ~0.01 mg/L; https://www.epa.gov/dwreginfo/chemical-contaminant-rules). Thermal waters in volcanic areas contain As concentrations that are often orders of magnitude higher than the EPA drinking water standard, and these elevated concentrations adversely impact downstream water resources worldwide (Ballantyne and Moore, 1988; López et al., 2012; Morales-Simfors et al., 2020; Nordstrom, 2002; Smedley and Kinniburgh, 2002; Webster and Nordstrom, 2003). For example, elevated As concentrations in thermal waters were measured in El Tatio, Chile (≤48 mg/L; Ballantyne and Moore, 1988; Landrum et al., 2009), Los Humeros, Mexico (≤74 mg/L; López et al., 2012), Lassen Volcanic National Park, California, United States of America (USA) (≤27 mg/L; Thompson et al., 1985), Valles Caldera, New Mexico, USA (≤18 mg/L; Goeff and Gardner, 1994), Campanian Volcanic Province, Italy (≤11 mg/L; Aiuppa et al., 2006), and Kamchatka, Russia (≤10 mg/L; Ellis and Mahon, 1977). Arsenic concentrations are also elevated in thermal waters of the Yellowstone Plateau Volcanic Field (YPVF), USA (≤17 mg/L; McCleskey et al., 2022), although most concentrations are in the range of 0.005 to 4 mg/L. Arsenic from thermal springs can potentially degrade downstream water quality (Garelick et al., 2008; Reid et al., 2003; Webster and Nordstrom, 2003) and thus, improved understanding of the biotic and abiotic processes controlling As fate and transport is needed to minimize risk to public health.

The YPVF covers an area of about ~17,000 km^2, most of which lies within and to the west of Yellowstone National Park (YNP). The YPVF provides a unique natural laboratory to characterize sources of As and the processes that control As concentrations, speciation, and transport with its more than 10,000 thermal features including hot springs, pools, geysers, mud pots, and fumaroles that have diverse chemical compositions (Allen and Day, 1935; Fournier, 1989; Hurwitz and Lowenstern, 2014; Lowenstern et al., 2015). Many studies have characterized As concentrations, speciation, As minerals, and biotic processes in the YPVF hydrothermal system (e.g., Ball et al., 2010; Donahoe-Christiansen et al., 2004; Gihring et al., 2001; Hague, 1911; Inskeep et al., 2004; Langner et al., 2001; Macur et al., 2004; McCleskey et al., 2014; Planer-Friedrich et al., 2006; Planer-Friedrich et al., 2007; Qin et al., 2009; Stauffer et al., 1980; Stauffer and Thompson, 1984; Weed and Pirsson, 1891). A network of gages in the major rivers draining YNP, within the YPVF (Fig. 1), measures water discharge continuously every 15 minutes (U.S. Geological Survey, 2021). Water discharge combined with specific conductance measurements used as a proxy for As concentrations (e.g. McCleskey et al., 2012) allows for quantification of fluvial As fluxes from YNP. Furthermore, fluvial transport of As in the YPVF appears to be minimally attenuated over long distances (McCleskey et al., 2010; McCleskey et al., 2019b; Nimick et al., 1998; Thompson, 1979). As a result, high fluvial As concentrations affect downstream water resources (Johnson, 2016; Miller et al., 2004; Montana Department of Environmental Quality, 2018; Nimick et al., 1998) and may affect plants, wildlife, and fish populations (Chaffee et al., 2007; Goldstein et al., 2001; Kocar et al., 2004; Robinson et al., 2006).

The YPVF is the location of three major caldera-forming eruptions that formed the Island Park caldera (2.1 Ma), Henry's Fork caldera (1.3 Ma), and the Yellowstone caldera (0.63 Ma,

Fig. 1) (Christiansen, 2001). In addition, there have been many large rhyolitic lava flows and tuff deposits within the YPVF, with the most recent occurring about 70,000 years ago. The YPVF is characterized by extensive seismicity, episodes of ground uplift and subsidence (Smith et al., 2009), and extremely high heat flow (Farrell et al., 2014; Hurwitz et al., 2012a). Additionally, a large reservoir of partially molten rhyolite beneath the YPVF (Farrell et al., 2014) at a depth of about 5 to 10 km (Fig. 2), fuels an extensive hydrothermal system that consists of a large number of geysers and numerous pools, springs, fumaroles, mud pots, and frying pans (Fournier, 1989; Hurwitz and Lowenstern, 2014). Groundwaters rise towards the surface and discharge mainly along fractures and terminations of rhyolite flows and tuff boundaries (Fig. 2, Hurwitz et al., 2020). Most thermal areas are within, or near the outer margins of the Yellowstone Caldera (Fig. 1), or along fault zones extending from the Caldera (Fournier, 1989; Hurwitz and Lowenstern, 2014).

The numerous pools, springs, fumaroles, mud pots, and frying pans in YPVF are frequently brightly colored, oftentimes due to the presence of pigments associated with phototrophic bacteria (oxygenic Cyanobacteria and a variety of anoxygenic bacteria) and Eukarya (algae) that are used to convert light energy to chemical energy and fuel their metabolisms (Brock, 1994). These colors can also be attributed to minerals, including the yellow- to red- colored As-containing minerals orpiment and realgar (Weed and Pirsson, 1891). In circumneutral to alkaline (mostly neutral-Cl and Cl-rich waters) thermal springs in the YPVF, photosynthetic microbial life is restricted to waters with a temperature of <73°C and in acidic springs (primarily acid-SO_4 and Cl-SO_4 rich waters), photosynthetic life is restricted to an even lower temperature of <54°C (Boyd et al., 2012; Cox et al., 2011; Fecteau et al., 2022; Hamilton et al., 2012). Thus, at temperatures >73°C in circumneutral to basic springs or >54°C in acidic

springs, microbial life is not supported by light energy but rather by chemical energy released through oxidation-reduction reactions involving inorganic electron donors and acceptors that are in disequilibrium (Amend and Shock, 2001; Shock et al., 2010). As outlined above, among the most common inorganic electron donors and acceptors available to chemosynthetic microbial life in hot springs in the YPVF are As compounds. In utilizing As species to drive their energy metabolism, microorganisms transform these substrates in ways that affect their speciation, solubility, toxicity, and mobility.

The goals of this study are to synthesize and interpret As data collected by the U.S. Geological Survey over several decades to provide an overview of As sources, the important geochemical and microbial processes affecting As speciation and concentration, and factors affecting As transport in the YPVF. Microbial processes have long been known to transform aqueous As speciation and its consequent toxicity and mobility (Stolz et al., 2006; Zhu et al., 2014). We attempt to integrate the current understanding of microbial processes with the hydrochemistry to provide a more complete description of As dynamics in the YPVF. Many of the geochemical and microbial processes controlling As concentrations, redox state, speciation, and fluvial transport in YPVF may be applicable to hydrothermal systems around the world.

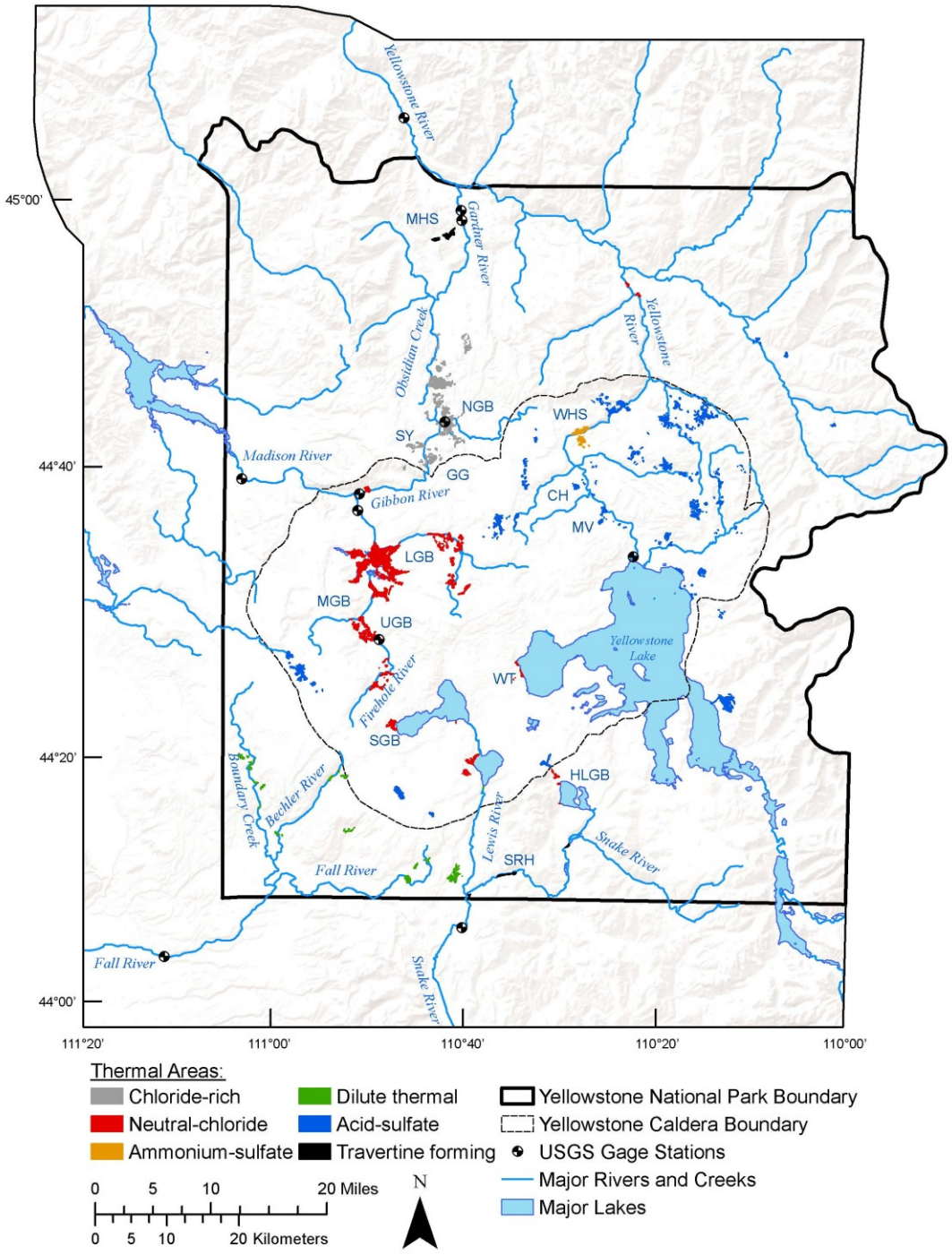

Figure 1. Map of the Yellowstone Plateau Volcanic Field with the thermal areas identified by predominant thermal water type. Location of thermal areas are from Vaughan et al. (2013). The following major thermal areas are identified: Mammoth Hot Springs (MHS), Norris Geyser

Basin (NGB), Sylvan Hot Springs (SY), Gibbon Geyser Basin (GG), Lower Geyser Basin (LGB), Midway Geyser Basin (MGB), Upper Geyser Basin (UGB), Shoshone Geyser Basin (SGB), Snake River Hot Springs (SRH), Heart Lake Geyser Basin (HLGB), West Thumb Geyser Basin (WT), Mud Volcano (MV), Crater Hills (CH), and Washburn Hot Springs (WHS).

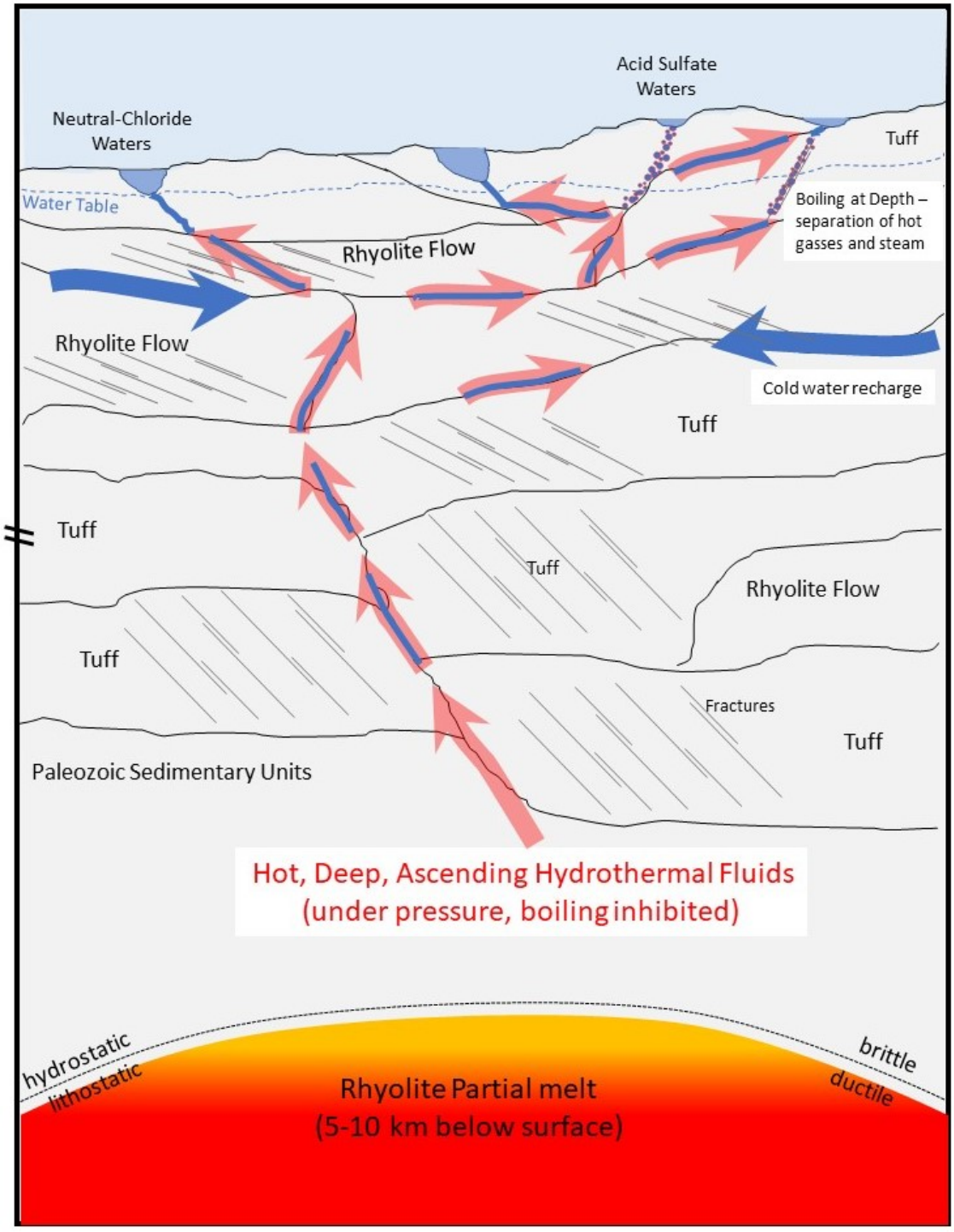

Figure 2. Conceptual diagram of water flow-paths in the Yellowstone Plateau Volcanic Field subsurface and formation of various thermal waters. Figure modified after Hurwitz et al. (2020)

and Webster and Nordstrom (2003). Vertical scale is approximated and for descriptive purposes only.

2. Datasets

Chemical analyses of thermal waters have been reported from nearly every thermal area in the YPVF (Allen and Day, 1935; Ball et al., 2010; Ball et al., 2006; Ball et al., 2002; Ball et al., 1998b; Bergfeld et al., 2019; Gemery-Hill et al., 2007; Gooch and Whitfield, 1888; Hurwitz et al., 2012b; Lowenstern et al., 2012; McCleskey et al., 2005; McCleskey et al., 2014; McCleskey et al., 2022; Stauffer et al., 1980; Thompson and DeMonge, 1996; Thompson and Hutchinson, 1981; Werner et al., 2008). Chemical analyses, including As and Cl, of rhyolites collected from the YPVF are reported in Harrison et al. (2022). Specific information about sample collection and chemical analyses can be found in each report. From these data reports, we compiled water chemistry data from ~1,800 water samples collected from pools, springs, geysers, and mud pots that include reported As concentrations (Ball et al., 2010; Ball et al., 2006; Ball et al., 2002; Ball et al., 1998b; Bergfeld et al., 2019; Gemery-Hill et al., 2007; Lowenstern et al., 2012; McCleskey et al., 2005; McCleskey et al., 2022). The dataset includes As concentrations that were below the method reporting limit up to 17 mg/L. Multiple samples from the same thermal feature were reduced to a single concentration by utilizing the geometric mean. For thermal water samples collected from a spring source and its drainage, only samples from the spring were included in the database. After vetting, As analyses from 391 thermal springs were obtained, of which 330 have GPS coordinates associated with the sample. Arsenic biogeochemistry of drainages is discussed separately from spring source water. For studies of As transformations along drainages, all the data from an individual spring and its drainage are used to interpret changes in As geochemistry. It is important to note that As(III) concentrations reported here were performed by hydride generation atomic absorption spectrometry (HGAAS) and the determinations are operationally defined as reduced As species (As(III)) that readily

form arsine by borohydride reduction including arsenite (H_3AsO_3) and likely methyl- and thio-As species (McCleskey et al., 2003; Planer-Friedrich and Wallschläger, 2009). Water chemistry data, including As and Cl, from a leaching experiment in which rhyolite was reacted with deionized water at 150 °C to 350 °C and 25 MPa was also utilized (Cullen et al., 2019).

3. Methods

3.1 Collection and analysis of water samples

For most of the samples utilized in this study (Ball et al., 2010; Ball et al., 2006; Ball et al., 2002; Ball et al., 1998a; Ball et al., 1998b; Bergfeld et al., 2019; Gemery-Hill et al., 2007; McCleskey et al., 2005; McCleskey et al., 2014; McCleskey et al., 2019a; McCleskey et al., 2022; Thompson and DeMonge, 1996), two general types of water samples were collected, thermal and river water. Specific sampling details are included within each publication. For most thermal water samples, water was pumped directly from the source with a battery-operated peristaltic pump fitted with Teflon tubing through a filter (≤0.45-micrometer (μm) pore size). For river and stream samples, water was filtered through a syringe filter (≤0.45 μm). Water samples collected for total dissolved As were preserved with nitric acid (1% v/v) and As redox species (McCleskey et al., 2004) were preserved with hydrochloric acid (1% v/v). For a small number of neutral-Cl samples that were elevated in sulfide and arsenite, it is thought that poorly crystalline As_2S_3 formed upon acidification with HCl resulting in a loss of dissolved arsenite (Smieja and Wilkin, 2003). Using the procedure described by McCleskey et al. (2014), arsenite (As(III)) concentrations in neutral-Cl water samples that were impacted by As_2S_3 precipitation were not included in these analyses.

Given the long period of water-chemistry studies in Yellowstone and the advancements in analytical instrumentation, a variety of As analytical methods were utilized. Regardless of methodology utilized, most of the reported As concentrations appear to be reliable based on the chemical relationships utilized in this study. For water samples collected and analyzed in the 1970's, ultraviolet/visible spectrophotometry was used to determine concentrations of As(III) and As(V) (Stauffer, 1980; Stauffer et al., 1980; Stauffer and Thompson, 1984). For water samples collected in the 1980's, As was determined by atomic-emission spectroscopy in a direct-current argon plasma (Thompson and DeMonge, 1996). Beginning in the 1990's, total dissolved As concentrations in nitric acidified samples were determined using inductively coupled plasma atomic emission spectroscopy (ICP-OES) and hydride-generation atomic absorption spectrometry (HGAAS) was used to measure total dissolved As (As(T)) and dissolved arsenite (As(III)) concentrations in hydrochloric acid acidified samples (Ball et al., 2010; Ball et al., 2006; Ball et al., 2002; Ball et al., 1998a; McCleskey et al., 2005; McCleskey et al., 2014). The uncertainty for analytical determinations used in this study is expected to be less than 5 to 10% for concentrations that are greater than 10 times the method detection limit. The uncertainty may be larger than 10% for those samples with concentrations less than 10 times the method detection limit.

The As flux, or the mass of As per unit time at any given site, was determined at YPVF river monitoring sites located at or near USGS gages (Fig. 3). In addition, instantaneous As flux measurements have been determined during low-flow (September) synoptic studies at numerous sites throughout YPVF. Solute flux is the product of solute concentration, discharge, and a unit conversion factor integrated over time. For the continuous monitoring sites, specific conductance is used as a proxy for As concentrations at eight river and creek monitoring sites within the

YPVF (McCleskey et al., 2012; McCleskey et al., 2020; McCleskey et al., 2016; McCleskey et al., 2019b). The specific conductance monitoring sites are located near USGS gages where discharge and specific conductance data are collected concurrently every 15 min (McCleskey et al., 2019c; U.S. Geological Survey, 2021). The specific conductance-As concentration correlations were determined using the following equation:

$$C = a \cdot SC + b \quad (1)$$

where C is the As concentration (mg/L), a is a site- and As-specific linear coefficient, SC is the specific conductance (μS/cm), and b is a site and As-specific intercept. Updated specific conductance-solute concentration correlations are presented here using numerous water samples and specific conductance measurements collected from each of the long-term monitoring sites over almost the entire hydrological and geochemical range. For each of the monitoring sites, the specific conductance, chemical data, and field and analytical methods are reported in McCleskey et al. (2019c). Instantaneous fluvial As concentrations and fluxes obtained from four different synoptic studies are combined here to provide an overview of As sources and mass transport in YPVF (McCleskey et al., 2012; McCleskey et al., 2020; McCleskey et al., 2016; McCleskey et al., 2010). Sample locations and field and analytical details are provided in each of the referenced studies.

3.2 Rock sample analysis

Arsenic concentrations were measured in YPVF rhyolite samples by three different methods. The first method involved complete digestion using strong acids (hydrofluoric acid, nitric acid, and hydrochloric acid mixture) and heating with a microwave. The samples were then evaporated to dryness and redissolved using nitric acid (Harrison et al., 2022). These samples

were analyzed by ICP-MS (Roth et al., 2022). Chloride concentrations were measured in seventeen YPVF rhyolite samples using strong acid (hydrofluoric acid and nitric acid mixture) digestion, heating with a microwave, and analyses by ICP-MS (Roth et al., 2022). The second method was wavelength dispersive X-ray fluorescence spectrometry (WD-XRF) performed at the Hamilton Analytical Laboratory in Hamilton College, New York (Harrison et al., 2022). The third method was by Laser Ablation Inductively Coupled Plasma Mass Spectrometry (LA-ICP-MS) at the Colorado School of Mines (CSM) in Golden, Colorado (Harrison et al., 2022). Rhyolite pellets (15-mm) were mounted on a one-inch glass puck and used for both the WD-XRF and the LA-ICP-MS analyses. The WD-XRF analyses followed the methods described by (Finkelshtein and Chubarov, 2010) and (Uhlig et al., 2016) and quantified As and Cl concentrations. The LA-ICP-MS quantified their major and trace element chemistry, including As, using the Applied Spectra Resolution-SE 193nm ArF excimer laser ablation system at the CSM Laboratory (for additional details see Churchill et al., 2021b). All sample glasses were each ablated two times during a run, with 1,000 μm by 150 μm tracks. A custom fused low dilution drift monitor was ablated frequently throughout the approximately seven-hour run to correct for drift.

3.3 Microbiological Methods

The distribution of proteins putatively involved in select As transformations in hot spring microbial communities was assessed by identification of all proteins encoded in community metagenomes. Metagenomes were generated by shotgun sequencing of DNA that was extracted from microbial communities associated with hot spring sediments. Since all metabolic functions are encoded in the genomes of resident populations, metagenomes represent the functional

potential of microbial communities, and these functions can be inferred by identifying proteins encoded in the metagenomic DNA.

Three principal enzymatic systems are currently known to catalyze the transformation of As compounds to allow the conservation of energy in Bacteria and Archaea, including those that 1) oxidize arsenite coupled to aerobic respiration (e.g., coupled to O_2 reduction), 2) those that oxidize arsenite coupled to anaerobic respiration (e.g., reduction of non-oxygen compounds like nitrate, NO_3), and 3) those that allow reduction of arsenate coupled to the use of reductants like organic carbon or inorganic electron donors. The three principal enzyme systems that catalyze these reactions are all evolutionarily related and belong to the dimethyl sulfoxide-molybdopterin (DMSO-M) oxidoreductase family of proteins that are involved in numerous microbial oxidation/reduction reactions of inorganic substrates. Thus, the potential for As transformation by DMSO-M enzymes can be assessed by identifying proteins encoded in metagenomic sequence based on the similarity (i.e., homology) to catalytic subunits of DMSO-M complexes that have been previously characterized (Kumari and Jagadevan, 2016; McEwan et al., 2002). Previously compiled databases of DMSO-M oxidoreductase arsenite oxidase large subunits (AioA), anaerobic arsenite oxidases (ArxA), and arsenate reductases (ArrA) (Danczak et al., 2019; Zargar et al., 2012) were used to identify the three aforementioned protein families within 32 previously compiled YPVF hot spring community metagenomes (Colman et al., 2020). In addition, the presumed arsenate reductase DMSO-M for *Pyrobaculum* strains (e.g., Pars_0389 for *Pyrobaculum arsenaticum;* termed ArrA-like here) (Cozen et al., 2009) was used to identify divergent arsenate reductase-like proteins within the metagenomes, following previous identification of ArrA-like proteins (Jay et al., 2015; Muramatsu et al., 2020). The community

metagenomes used to analyze protein distribution are the same as in Colman et al. (2020) that derive from multiple studies across a wide range of thermal water types in the YPVF.

Briefly, all sediment samples used were frozen in the field and transported frozen back to the lab where they were thawed and subjected to whole community DNA extraction, followed by shotgun metagenomic sequencing of DNA fragments and protein annotation (Colman et al., 2020). Additional information including field geochemical parameters that were available for all springs and locations are provided in Supplementary Table S1.

Initial BLASTp searches were conducted with representative arsenite oxidase and arsenate reductase proteins (using the large catalytic subunits of each complex) against the metagenome database, with putative oxidases/reductases identified by >30% amino acid identity and >60% query coverage to reference protein sequences (Altschul et al., 1990). The putative oxidases/reductases were then aligned using the Clustal omega sequence alignment program (Sievers et al., 2011) with the above reference datasets and then subjected to Maximum-Likelihood phylogenetic analyses with the IQ-TREE program (Nguyen et al., 2015). Putative oxidases/reductases were identified based on monophyletic relationships with AioA, ArxA, ArrA, or Pars_0389 (ArrA-like). The reads per kilobase pair per million mapped read (RPKM) values for genes were calculated as the number of mapped sequences reads to metagenomic contig / (metagenomic contig length/1,000 x total reads in the metagenome / 1,000,000). Read mapping was conducted as described in Colman et al. (2020). Values for individual genes were summed across all oxidase or reductase genes for a given spring community genome to calculate a summed relative abundance value for arsenite oxidases (aerobic and anaerobic) or arsenate reductases (ArrA and Arra-like). The taxonomic identities of putative oxidases/reductases were

determined based on BLASTp searches (Altschul et al., 1990) against the NCBI nr database (Sayers et al., 2022).

4. Arsenic concentrations in thermal waters

The distribution of As concentrations for 330 individual thermal springs located in 30 different thermal areas across YPVF is shown in Fig. 3 (Ball et al., 2010; Ball et al., 2006; Ball et al., 2002; Ball et al., 1998b; Bergfeld et al., 2019; Gemery-Hill et al., 2007; Lowenstern et al., 2012; McCleskey et al., 2005; McCleskey et al., 2022). Most As concentrations in YPVF thermal springs are in the range of 0.005 to 4 mg/L, but As can vary substantially with water type (Fig. 4a). The main thermal water types in YPVF include neutral-Cl, acid-SO_4, carbonate-rich waters, and mixtures of these. The formation of these thermal water types depends on subsurface lithology (rhyolites, basalts, and sedimentary deposits), temperature, residence time, amount of boiling, mixing of thermal waters and groundwaters, amount of ingassing and degassing, amount of precipitation and dissolution of secondary As minerals, and incorporation into sinter (Hurwitz and Lowenstern, 2014; López et al., 2012; Morales-Simfors et al., 2020; Sanchez-Yanez et al., 2017; Webster and Nordstrom, 2003). Ellis and Mahon (1964, 1977) demonstrated the importance of hydrothermal leaching of rocks to obtain the water compositions of hot springs and geysers. To understand why As concentrations vary across the YPVF, it is necessary to describe subsurface water-rock interactions and processes that lead to the various thermal waters. Throughout much of the YPVF, thermal waters emerge from rhyolite flows and tuffs (Hurwitz et al., 2020); however, outside the Yellowstone Caldera, thermal waters emerge from rhyolite tuffs (Norris Geyser Basin), limestones (Mammoth Hot Springs), and alluvial and glacial deposits (Mud Volcano). Figure 2 shows a schematic of potential thermal water flow paths and physical

processes (e.g., boiling and separation of volatiles). A widely accepted model for the genesis of most thermal waters in YPVF includes a deep, hydrothermal reservoir (Fournier, 1989) that is recharged by infiltrating meteoric water. Deep hydrothermal fluids are pressurized and, thus, contain high concentrations of dissolved gases, including carbon dioxide (CO_2) and hydrogen sulfide (H_2S) (Lowenstern et al., 2015). The deep thermal waters rise toward the surface through fractures. As the fluids rise, pressure decreases, and the boiling point of water is reached. For some neutral-Cl springs, boiling occurs near or at the surface. When boiling occurs at depth, steam rich in gases (e.g., CO_2 and H_2S) separates from the thermal water, concentrating solutes in the remaining parent water (e.g., as is the case for Cl-rich thermal waters from Norris Geyser Basin). The separated gases and heat can subsequently mix with shallow oxic groundwaters and H_2S oxidizes to form sulfuric acid (H_2SO_4) creating acid-SO_4 waters (Fig. 2).

Elevated As concentrations are common in neutral-Cl thermal waters (1.2 ± 0.8 mg/L; Fig. 1 and 4a) in the western part of the Yellowstone Caldera (e.g., springs in Upper, Midway, Lower, Shoshone, and West Thumb Geyser Basins) where they primarily emerge through rhyolite lava flows. Neutral-Cl thermal waters have near neutral to alkaline pH (Nordstrom et al., 2009) and usually deposit sinter (Churchill et al., 2021a). The pH of neutral-Cl thermal waters measured at the surface range from circumneutral to basic (up to ~ pH 9.5) because the pH increases with CO_2 degassing. Neutral-Cl groundwaters are typically near the local boiling point (some are superheated) at the ground surface, equilibrate with rhyolite at temperatures estimated to be between 170°C to 220°C (Fournier, 1977; Fournier, 1989; King et al., 2016; White et al., 1988), have large discharges compared to acid-SO_4 waters, and are characterized by relatively high concentrations of Cl, SiO_2, Na, Li, and B (Fournier, 1989; Hurwitz and Lowenstern, 2014).

Springs with relatively low As concentrations include acid-SO_4, NH_4-SO_4 rich, and dilute thermal waters (Fig. 4a). Acid-SO_4 thermal waters are shallow groundwaters that have been mixed with high temperature gases (CO_2, H_2S, and $H_2O(g)$) that exsolved from boiling of thermal waters at depth (Fig. 2, Fournier, 1989). These springs have low-pH (most are less than pH 4), high SO_4 concentrations (>100 mg/L) due to oxidation of H_2S forming H_2SO_4, and relatively low Cl concentrations (Nordstrom et al., 2009). These Cl and As poor waters are mainly steam condensates (White et al., 1971). Acid-SO_4 springs shape the surrounding landscape, which is typically barren and composed primarily of clays and resilient quartz grains. Acid-SO_4 springs are widespread in vapor-dominated thermal areas in the northeastern side of the caldera (Fig. 3) including Mud Volcano and Crater Hills, where steam and gases discharge from fumaroles, mud pots, and boiling pools with little to no discharge (Fournier, 1989; White et al., 1975), allowing for evaporation and concentration of H_2SO_4 (Nordstrom et al., 2009). The NH_4-SO_4 springs from Washburn Hot Springs (WHS, Fig. 3 and 4a) also contain relatively low As concentrations. Thermal waters from Washburn Hot Springs are derived from the distillation of glacial and lacustrine sediments which concentrates some volatile solutes including NH_4, where concentrations as high as about 900 mg/L have been measured (Ball et al., 2010; Ball et al., 1998a; Holloway et al., 2011). The NH_4-SO_4 waters contain low concentrations of Cl (3 ± 4 mg/L) and As (0.003 ± 0.007 mg/L, Fig. 4a). Dilute thermal waters are groundwaters that are conductively heated by rocks and steam that is depleted of H_2S or that are mixed with a small amount of neutral-Cl waters. Dilute thermal waters that have circumneutral pH and are relatively low in Cl, SO_4, and As (0.0001 to 0.4 mg/L; Fig. 4a). Many of the thermal springs in Southwest YPVF, including those along Boundary Creek and Bechler River (Fig. 3), are considered dilute

thermal waters that form as heat and steam originating from the Yellowstone Caldera are advected laterally and mix with non-thermal ground waters (Hurwitz et al., 2020).

Travertine-forming thermal waters with moderate As concentrations (0.4 ± 0.2 mg/L; Fig. 4a) are found at Mammoth Hot Springs and Snake River Hot springs (Fig. 1 and 3). Carbonate-rich thermal waters flow to the surface through sedimentary rocks (primarily limestone and gypsum-bearing shales) often forming travertine terraces found at Mammoth and Snake River Hot Springs (Fig. 3; Bargar, 1978; Fouke et al., 2000; Love and Keefer, 1975). These waters, often referred to as travertine-forming thermal waters, tend to have lower reservoir temperatures (100-120°C; Fournier, 1989) and lower concentrations of Cl and SiO_2 and higher concentrations of Ca, Mg, SO_4, and alkalinity compared to neutral-Cl waters (Fournier, 1989; Hurwitz et al., 2020). The pH of travertine-forming waters ranges from 6.2 to 7.0 and is buffered by the dissolution of limestone. The discharge from many travertine-forming thermal waters can be large (e.g., Boiling River).

Thermal waters from basins located near the Caldera boundary (e.g., Norris Geyser Basin, Sylvan Springs, Gibbon Geyser Basin, West Nymph Creek Thermal Area, and Heart Lake Geyser Basin; Fig. 3) contain a variety of thermal water types including acid-SO_4 with low As concentrations and Cl-rich thermal waters with high As concentrations (1.9 ± 1.2 mg/L; Fig. 4a). Springs from basins near or outside the caldera boundary (termed here "Cl-rich" Fig. 4a) are chemically distinct from neutral-Cl waters from within the caldera. Chloride-rich springs contain higher Cl and/or SO_4 concentrations than the neutral-Cl springs within the Caldera and many are acidic (White et al., 1988). Consequently, the distribution of Cl and As in Norris Geyser Basin thermal water also varies greatly. The highest As concentration that we have measured in YPVF was 17 mg/L in an unnamed large pool in the Ragged Hills area of Norris Geyser Basin

(McCleskey et al., 2022). The geometric mean As concentration in this unnamed pool was 3.3 mg/L for 34 samples collected from 2001 to 2018, and the peak measurement of 17 mg/L was likely the result of the dissolution of near-surface As rich soils as the bank around the pool appeared to have recently collapsed.

Another thermal area with disparate water types is Crater Hills, which is in the northeastern part of the YPVF (Fig. 3, CH). As mentioned above, most of the springs in the northeastern portion of the Caldera are vapor-dominated thermal waters. However, Sulphur Spring and nearby springs in Crater Hills have the highest Cl concentrations and geothermometer temperatures (270 to 300 °C) in the YPVF (Fournier, 1989). This spring appears to represent the most direct upward leakage of fluid from deep in the system (Fournier, 2005). Sulphur Spring contains some of the highest As concentrations (up to 6.5 mg/L) in YPVF and has undergone extensive boiling at depth and surface evaporation, and is enriched in H_2S gas that together result in higher Cl (>500 mg/L) and SO_4 (>300 mg/L) concentrations. Apart from the one sample collected in the Ragged Hills area of Norris Geyser Basin, the As concentration in Sulphur Spring and nearby springs (5.4 ± 0.9 mg/L; Fig. 4a) in Crater Hills are some of the highest in YPVF.

In thermal areas containing mixed water types, acid-SO_4 waters containing lower As concentrations are often found at higher elevations. For example, in the West Nymph Creek Thermal Area (WNCTA, Fig. 3) many thermal springs found on the north end of the basin, which are at higher elevations, tend to have lower As concentrations than springs that occur at lower elevations in the south. Similarly, Heart Lake Geyser Basin (HLGB, Fig. 3) contains both acid-SO_4 and neutral-Cl waters (Lowenstern et al., 2012). The northern most group of thermal springs in HLGB is at the higher elevation and contains acid-SO_4 waters with low As

concentrations; whereas the southern group emerge downgradient and contains mainly neutral-Cl waters with higher As concentrations (Fig. 3).

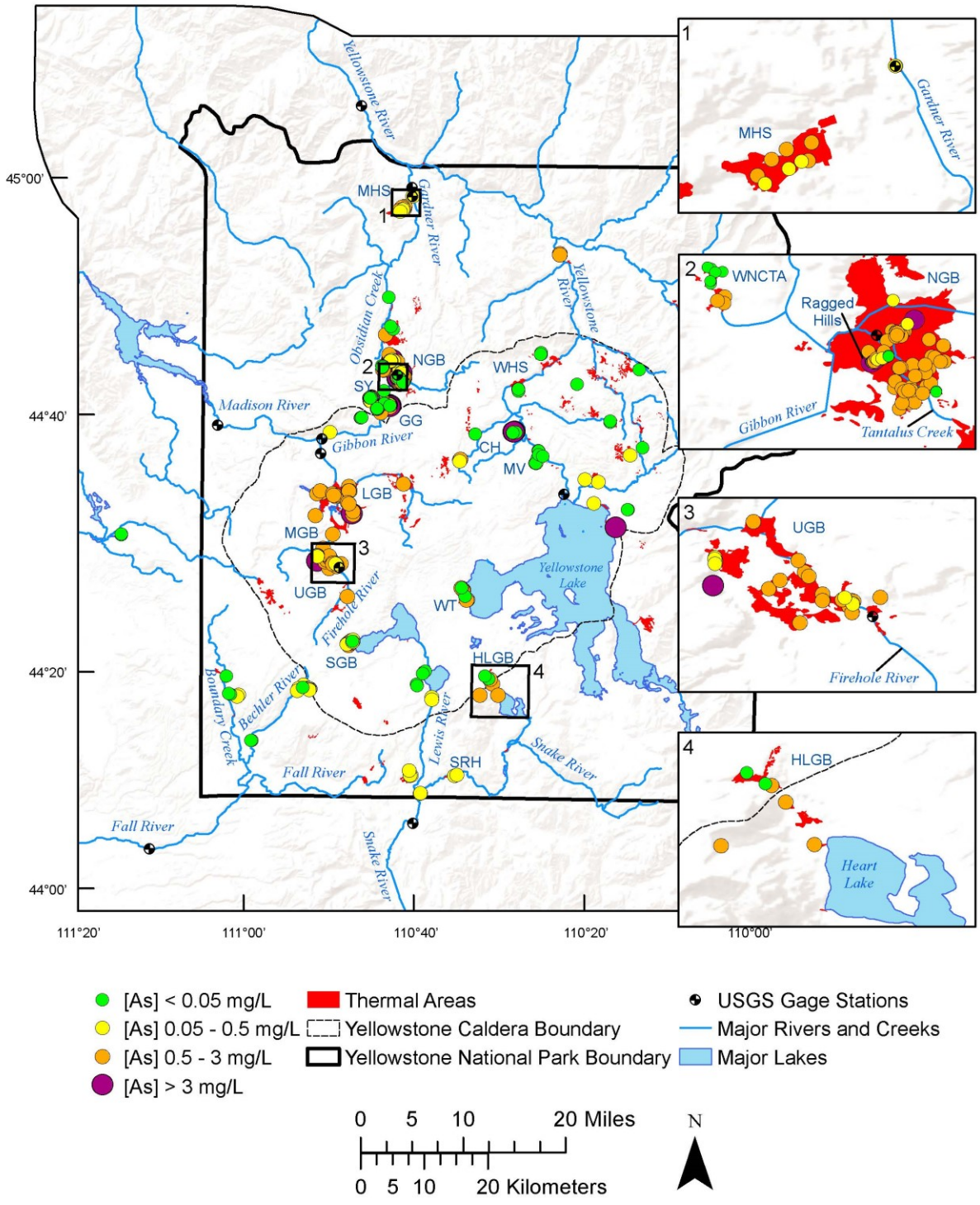
45°00'
44°40'
44°20'
44°00'
111°20'
111°00'
110°40'
110°20'
110°00'
Yellowstone River
Gardner River
Obsidian Creek
Madison River
Gibbon River
Yellowstone Lake
Firehole River
Boundary Creek
Bechler River
Fall River
Lewis River
Snake River
Heart Lake
Tantalus Creek
Ragged Hills
MHS
NGB
WNCTA
WHS
SY
GG
CH
MV
LGB
MGB
UGB
WT
SGB
HLGB
SRH
1
2
3
4
[As] < 0.05 mg/L
[As] 0.05 - 0.5 mg/L
[As] 0.5 - 3 mg/L
[As] > 3 mg/L
Thermal Areas
Yellowstone Caldera Boundary
Yellowstone National Park Boundary
USGS Gage Stations
Major Rivers and Creeks
Major Lakes
0 5 10 20 Miles
0 5 10 20 Kilometers
N

Figure 3. Arsenic concentrations in Yellowstone Plateau Volcanic Field thermal waters represented by colored dots. The following major thermal areas are identified: Mammoth Hot Springs (MHS), Norris Geyser Basin (NGB), Sylvan Hot Springs (SY), Gibbon Geyser Basin (GG), Lower Geyser Basin (LGB), Midway Geyser Basin (MGB), Upper Geyser Basin (UGB), Shoshone Geyser Basin (SGB), Snake River Hot Springs (SRH), Heart Lake Geyser Basin (HLGB), West Thumb Geyser Basin (WT), Mud Volcano (MV), Crater Hills (CH), Washburn Hot Springs (WHS), and West Nymph Creek Thermal Area (WNCTA). Data used in this figure are from Ball et al., 2010; Ball et al., 2006; Ball et al., 2002; Ball et al., 1998b; Bergfeld et al., 2019; Gemery-Hill et al., 2007; Lowenstern et al., 2012; McCleskey et al., 2005; and McCleskey et al., 2022.

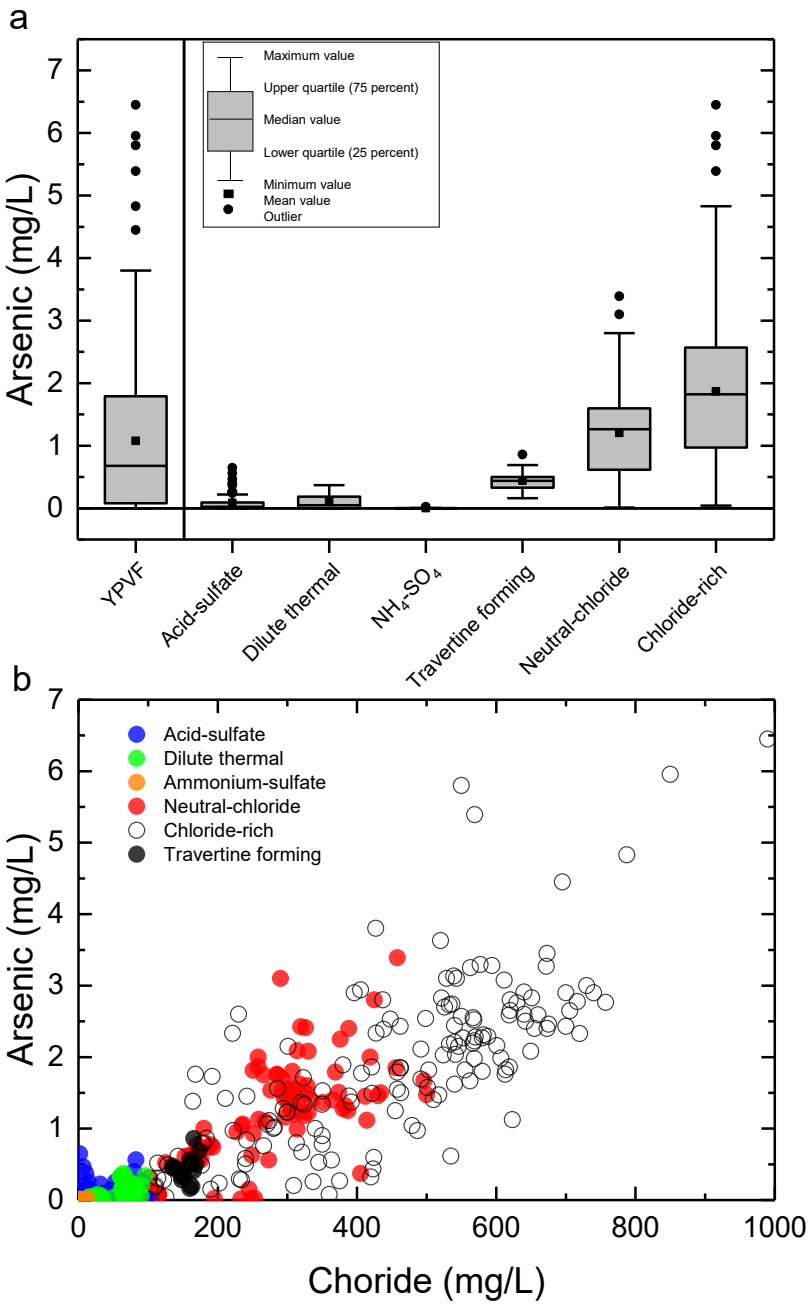

Figure 4. Box plot of As concentrations in Yellowstone Plateau Volcanic Field thermal waters and the six thermal water types used in this study (a) [maximum value = (upper quartile) + inner quartile x 1.5; minimum value = (lower quartile) + inner quartile x 1.5]. Plot of As against Cl

concentrations (b). Data used in this figure are from Ball et al., 2010; Ball et al., 2006; Ball et al., 2002; Ball et al., 1998b; Bergfeld et al., 2019; Gemery-Hill et al., 2007; Lowenstern et al., 2012; McCleskey et al., 2005; and McCleskey et al., 2022.

4.1 Arsenic sources and water-rock interactions

The source of As can be inferred from the hot spring's chemical composition. For YPVF thermal waters, solute concentrations and behavior relative to Cl (Fig. 4b) are often utilized to infer sources and reactivity because the vast majority of Cl in YPVF is derived from high temperature leaching of large volumes of rhyolite and Cl behaves conservatively throughout the system (Cullen et al., 2019; Cullen et al., 2021; Feth, 1981). Although distinguishing between Cl degassed from magma and Cl leached from rhyolites into the hydrothermal system is difficult, further evidence for limited magmatic Cl in the YPVF hydrothermal system is based on calculations showing that a mixture of about 0.2–0.4 wt.% magmatic fluid with 99.6–99.8 wt.% meteoric water could account for all the discharged thermal Cl (Fournier, 1989). The slightly higher Cl/B values in neutral-chloride waters from YPVF (83 ± 18) compared to the ratio in YPVF rhyolite (70 ± 15) may suggest that a very small fraction of Cl from a different source, possibly from degassing of the underlying magma, and/or some loss of volatile B (Cullen et al., 2021). Stable Cl isotopes ($\delta^{37}Cl$) are relatively uniform in Yellowstone's thermal waters and do not provide information that can discriminate between different sources (Cullen et al., 2021). Arsenic in YPVF surface waters is primarily derived from deep thermal fluids (Nordstrom et al., 2005; Stauffer and Thompson, 1984) and since As concentrations are positively correlated with Cl for neutral-Cl and Cl-rich thermal waters (Fig. 4b), it follows that a large portion of As in neutral-Cl hot springs is derived from high temperature leaching of rhyolites (Ellis and Mahon, 1964; Ewers, 1977). Furthermore, As has been found to be higher in silicic volcanic rocks (e.g.,

rhyolite common to YPVF) than most other igneous rocks (Onishi and Sandell, 1955) and rhyolites are known to have significant As concentrations which can be leached into the groundwater (Morales et al., 2015). For twenty-three YPVF rhyolite samples, the As concentrations ranged from 1.4 to 13 µg/g (median concentration of 3.1 µg/g, Harrison et al., 2022).

Further evidence of the source of As in YPVF thermal waters can be obtained by comparing the As/Cl mass ratio in thermal waters and Yellowstone rhyolites. However, apart from a few studies (Onishi and Sandell, 1955), there are limited data on As and Cl concentrations in YPVF rhyolites. Recent laboratory experiments (Cullen et al., 2019) that reacted Yellowstone rhyolite and water at temperatures between 150 °C and 350 °C have shown that at temperatures ≥ 275 °C nearly all the Cl and As are leached from the rhyolite into solution (Fig. 5a). The As to Cl ratio in the experiments was mostly temperature independent (Cullen, 2020; Cullen et al., 2019). The median As/Cl mass ratio (Fig. 5b) for neutral-Cl and Cl-rich thermal waters (0.004±0.002) is similar to the leach experiments of YPVF rhyolites (0.003±0.001; Cullen, 2020; Cullen et al., 2019). However, the As/Cl determined in rhyolites suggests that some rhyolites may be enriched in As relative to Cl. Variations in As/Cl are the result of, at least in part, differences in lithology, reservoir temperature, degree of boiling, mixing with shallow groundwater, secondary mineral formation, and reaction with near-surface rocks (Ballantyne and Moore, 1988; Webster and Nordstrom, 2003). Stauffer and Thompson (1984) observed cases in which the As/Cl ratio decreased in thermal waters, which was attributed to As precipitation in secondary As minerals.

Secondary As minerals may control As concentrations in some areas. Orpiment (As_2S_3) and realgar (As_4S_4) have been reported in Yellowstone (Hague, 1887; Weed and Pirsson, 1891).

In the Ragged Hills area of Norris Geyser Basin (Fig. 3), yellow precipitates, thought to be amorphous orpiment mixed with elemental sulfur (Nordstrom et al., 2003), are found in small pools. Nearby, in the acidic thermal sediments, yellow, orange, and bright red precipitates occur within the top 2 to 3 centimeters of the sediment. Because both orpiment and sulfur precipitate from acidic waters (Ballantyne and Moore, 1988) this area captures and concentrates As. Dissolution and/or precipitation of As minerals can alter dissolved As concentrations and As/Cl ratios (Nordstrom et al., 2001). For example, the small pools with yellow precipitates in the Ragged Hills area have relatively high Cl concentrations (310-360 mg/L), but the As/Cl ratio (0.0005 ± 0.0003) is about an order of magnitude lower than other Cl-rich pools (Fig. 5). Incorporation of As into pyrite has also been observed in other geothermal systems (Aiuppa et al., 2006; Ballantyne and Moore, 1988). In the YPVF, As may have partitioned onto particulates in springs where pyrite actively formed (e.g., Cinder Pool in Norris Geyser Basin; Colman et al., 2022; Xu et al., 2000), but such measurements were not made. Arsenic has been found to co-precipitate with silica sinter in the Upper Geyser Basin around neutral-Cl springs. Concentrations are highest in newly formed sinter and they decrease with increasing sinter age and dehydration (Churchill et al., 2021a).

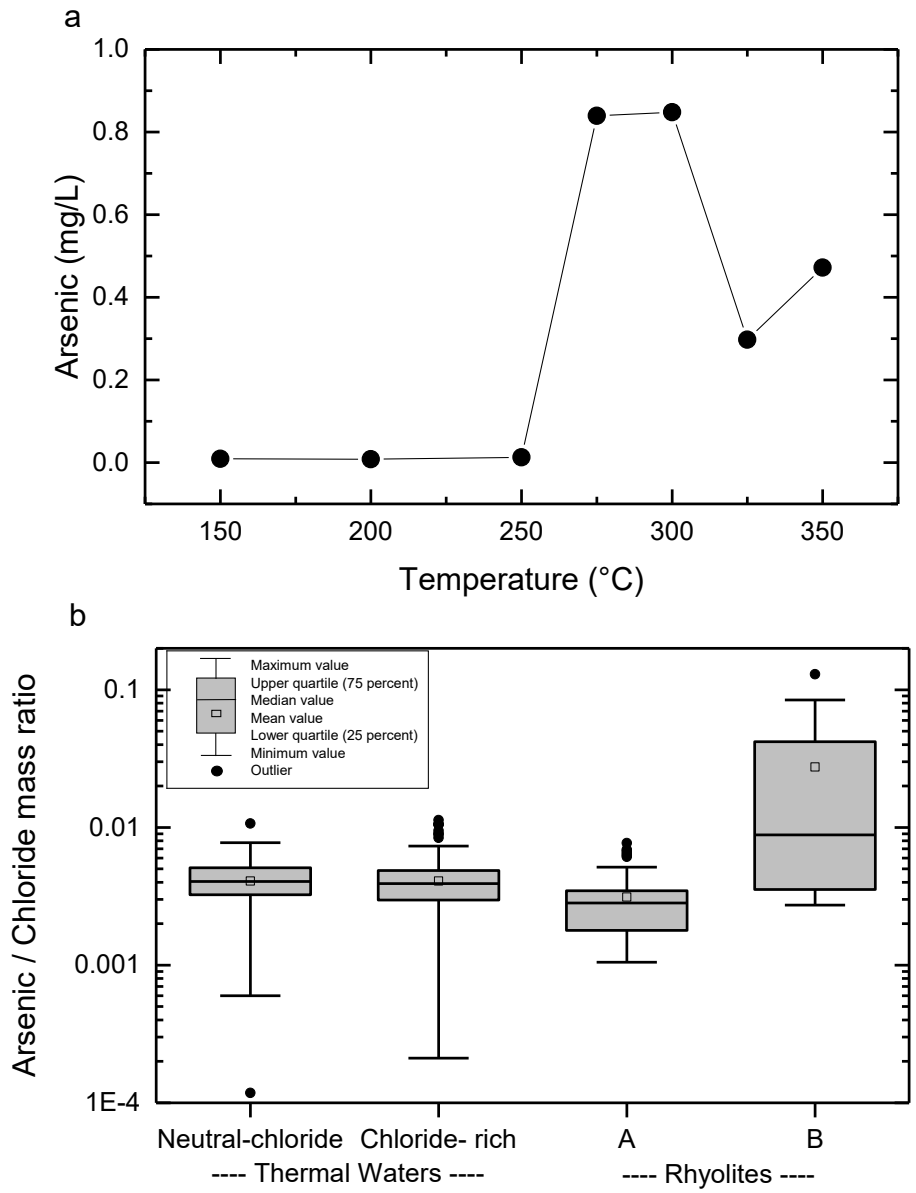

Figure 5. Plot of As leached from rhyolite at various temperatures (a). The data in (a) are from Cullen et al. (2019) and include the last sample collected at that temperature (91-95 days). Box plots of As/Cl mass ratio in neutral-Cl and Cl-rich thermal waters and Yellowstone rhyolites (b).

Rhyolite leach data (A) are from Cullen et al. (2019) and include data from all sample points and As data determined in rhyolites (B) determined using digestions and LA-ICP-MS (Harrison et al., 2022) [maximum value = (upper quartile) + inner quartile x 1.5; minimum value = (lower quartile) + inner quartile x 1.5]. The As/Cl ratio in thermal waters was determined using data from Ball et al., 2010; Ball et al., 2006; Ball et al., 2002; Ball et al., 1998b; Bergfeld et al., 2019; Gemery-Hill et al., 2007; Lowenstern et al., 2012; McCleskey et al., 2005; and McCleskey et al., 2022.

4.2 Processes controlling arsenic behavior

4.2.1 Geochemical and physical processes

Arsenic can be highly soluble in groundwaters depending on pH, redox conditions, temperature, and solution composition (Aiuppa et al., 2003; Nordstrom, 2002; Smedley and Kinniburgh, 2002). Similar to other thermal waters worldwide, the pH of the YPVF thermal waters have a bimodal distribution (Brock, 1971; Marini et al., 2003; Nordstrom et al., 2009): acidic (pH 1 to 5) and near neutral to basic (pH 5 to 10). However, As concentrations are not correlated with pH in YPVF thermal waters (Fig. 6a) and, therefore, pH does not appear to control As concentrations in this system. Worldwide, As is commonly concentrated in sulfide-bearing minerals (i.e., orpiment, pyrite, and arsenopyrite) and also in hydrous Fe oxides. The solubility of both sulfide minerals (pyrite) and Fe oxides, and thus As, often depends on pH and redox conditions (Nordstrom, 2002). In the YPVF, acid-SO_4 waters are typically generated from sulfur and sulfide oxidation following H_2S degassing from depth (Nordstrom et al., 2009), rather than pyrite oxidation. Consequently, metal concentrations, including iron, are much lower in the

YPVF thermal waters than in acid mine waters of similar pH (Nordstrom et al., 2009) and, thus, As concentrations in most YPVF waters are not pH or Fe dependent. Low Fe concentrations also allow for unattenuated transport of As in most YPVF river waters.

The various water types used in this study have distinctly different Cl and SO_4 concentrations (Fig. 6b), and, thus, initial insights into the processes influencing their As concentrations can be made on that basis (Nordstrom et al., 2009). The neutral-Cl thermal waters found in the western part of the Yellowstone Caldera (e.g., Upper, Midway, Lower, Shoshone, and West Thumb Geyser Basins) contain markedly lower Cl and/or SO_4 concentrations than the Cl-rich waters. Neutral-Cl waters boil at or near the surface and as a result the Cl and SO_4 concentrations are limited to less than ~500 and ~100 mg/L, respectively. Many neutral-Cl waters are similar in composition to the deep-seated hydrothermal water estimated by Fournier (2005). The Cl-rich springs located near the caldera boundary (e.g., Norris Geyser Basin, Sylvan Springs, Gibbon Geyser Basin, West Nymph Creek Thermal Area, and Heart Lake Geyser Basin; Fig. 3) contain markedly higher Cl and/or SO_4 concentrations than neutral-Cl waters (Fig. 6b). When boiling of waters occur at depth, steam and gases (CO_2 and H_2S) are volatilized, while Cl (>~500 mg/L) and As (often 2-4 mg/L; Fig. 4b) concentrations increase in the remaining fluid. Furthermore, only a small fraction of As (<0.5%) partitions into the steam phase (Ballantyne and Moore, 1988). Sulfate concentrations in many of these boiled waters are similar to neutral-Cl waters because a substantial portion of the sulfide in the waters (in the form of H_2S) has been exsolved from solution and is thus unavailable for oxidation which would further increase SO_4 concentrations (Nordstrom et al., 2009). The Cl-rich waters with high SO_4 concentrations (>~100 mg/L SO_4), did not boil or exsolve H_2S; thus, these waters contain higher SO_4 concentrations (due to the oxidation of H_2S), often lower pH (Fig. 6a.), and similar As concentrations as neutral-

Cl waters. For acid-SO_4 waters (Fig. 6b), the high SO_4 and low Cl and As concentrations represent meteoric waters that mixed with high temperature gases (rich in H_2S) that oxidized and formed sulfuric acid (Nordstrom et al., 2009). Dilute thermal waters are meteoric and heated by rocks and steam that is depleted of H_2S or that are mixed with a small amount of neutral-Cl waters. These waters contain low SO_4, Cl, and As concentrations (Fig. 6b). Sulfur Spring and nearby springs in Crater Hills contain some of the highest As (up to 6.5 mg/L), Cl, and SO_4 concentrations in the YPVF and appear to represent the most direct upward leakage of fluid deep in the system (Fournier, 2005). Many waters fall between the main water types because of mixing and/or various amounts of boiling. Finally, carbonate-depositing waters found in Mammoth and Snake River Hot Springs are also shown on Fig. 6b; however, much of the SO_4 in these spring waters is derived from the dissolution of gypsum-bearing shales and the pH (6.0 to 7.5) is buffered by the dissolution of limestone.

Stable water isotopes can provide additional insight into the chemical processes affecting As concentrations and the importance of evaporation on As concentrations. In Fig. 6c, As concentration is plotted against $\delta^{18}O$ for thermal waters from YPVF. An increase in $\delta^{18}O$ indicates more evaporation. For the neutral-Cl and Cl-rich thermal waters there are two important trends. First, for the neutral-Cl waters, As concentrations are positively correlated with $\delta^{18}O$ demonstrating the effects of evaporation on As concentrations. Second, many of the Cl-rich waters are more evaporated than neutral-Cl waters indicating additional boiling. Also, the As concentrations for many of the most evaporated Cl-rich samples (i.e., increasing $\delta^{18}O$) suggest mixing with acid-SO_4 waters. The $\delta^{18}O$ for dilute thermal waters indicate little evaporation and are reflective of warm dilute meteoric groundwaters free of As that are conductively heated by rocks or steam. The $\delta^{18}O$ for travertine-forming waters from Mammoth and Snake River Hot

Springs are similar and also indicate little evaporation or boiling, consistent with findings of Kharaka et al. (2000), indicating that Mammoth thermal water is mainly meteoric. The $\delta^{18}O$ values from acid-SO_4 and NH_4-SO_4 waters are generally isotopically heavy and are consistent with thermal springs with little discharge and high evaporation. Despite high evaporation, the As concentrations in acid-SO_4 and NH_4-SO_4 waters remain low because the infusing hot gasses lack substantial As concentrations.

Thermal waters in close spatial proximity tend to have similar As/Cl ratios and the As and Cl concentrations are either decreased by dilution with meteoric waters or increased due to boiling (Webster and Nordstrom, 2003). However, mixing of various water types is also an important process controlling water composition in the YPVF. Figure 6d is an example of two endmember mixing for an unnamed pair of co-localized hot springs in the Ragged Hills area of Norris Geyser Basin. The two springs are roughly the same diameter, ~ 2 m, located adjacent to each other, and are only separated by about 50 cm of silicified rock. Water samples were collected from the pools from 2005 through 2018 (Ball et al., 2010; Ball et al., 2006; McCleskey et al., 2014; McCleskey et al., 2022). In 2005, only one pool existed as the rock-bridge separating the pools had not formed. By 2006 the rock-bridge had formed, and two pools were evident. In 2007, the chemistry of the two springs were similar but beginning in 2009 we noticed that the chemistry of the two springs diverged. From 2009 to 2018, we collected 29 samples from these two springs (Fig. 6d). The East spring (pH 4.5 ± 1.2) is a Cl-rich spring with an average Cl concentration of 674 ± 44 mg/L, SO_4 concentration of 48 ± 24 mg/L, and As concentration of 2.8 ± 0.4 mg/L. The chemical composition of the West spring (pH 2.5 ± 0.5) is variable and appears to be a mixture of ~acid-SO_4 and East spring waters. It is unclear whether mixing of waters at this site occur in the subsurface, across the bridge, or both.

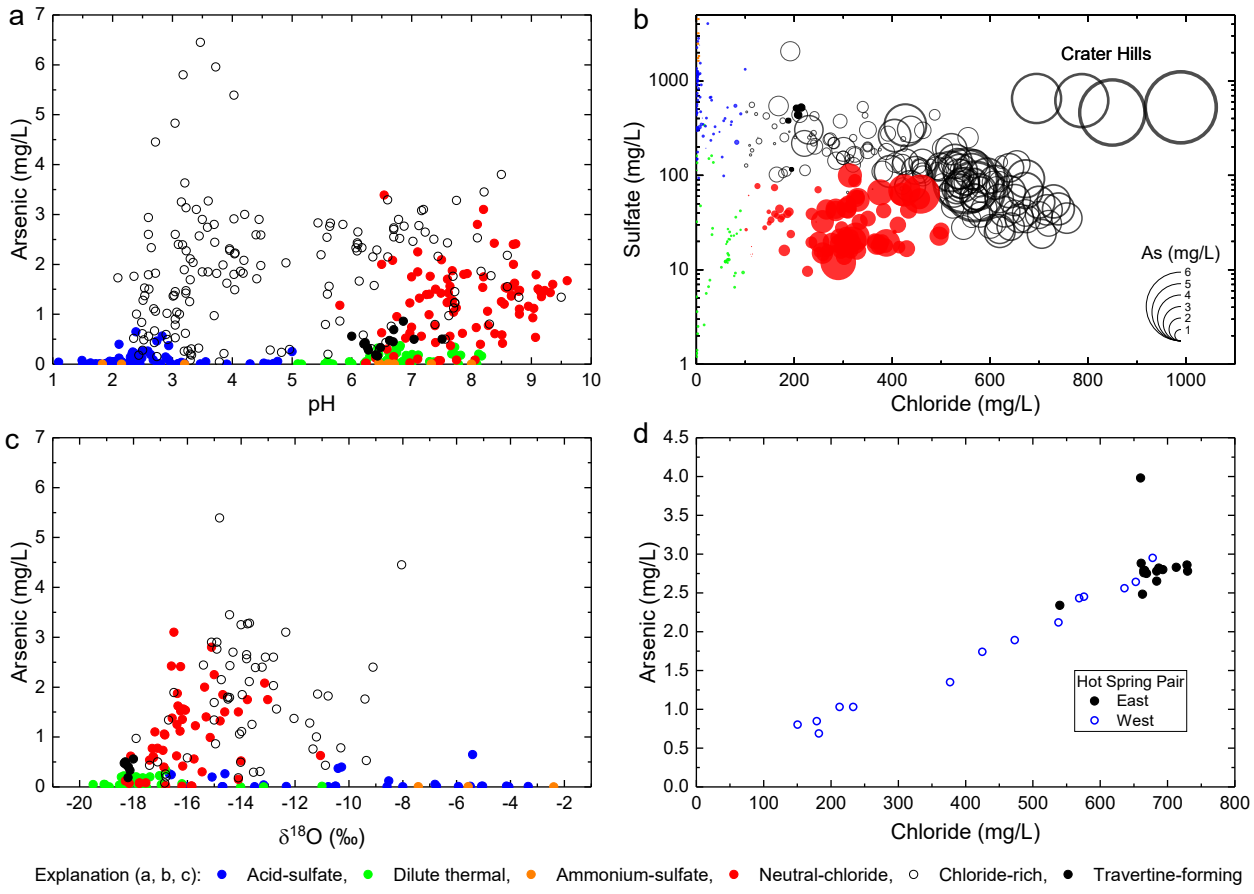

Figure 6. Plot of As in relation to pH (a). Bubble plot of SO_4 against Cl concentrations with the size of the bubble being representative of As concentrations (b). Plot of As against $\delta^{18}O$ of thermal waters (c). Plot of As against Cl concentration for an unnamed pair of hot springs that are co-localized in the Ragged Hills area of Norris Geyser Basin (d). Data used in this figure are from Ball et al., 2010; Ball et al., 2006; Ball et al., 2002; Ball et al., 1998b; Bergfeld et al., 2019; Gemery-Hill et al., 2007; Lowenstern et al., 2012; McCleskey et al., 2005; and McCleskey et al., 2022.

4.2.2 Arsenic oxidation states, speciation, and transformation

Deep thermal water contains reduced As (As(III)) (Ballantyne and Moore, 1988; Nordstrom et al., 2005). The presence of reduced sulfur species (H_2S and S_2O_3) inhibits the oxidation of As(III) to As(V) (Cherry et al., 1979) and abiotic oxidation of As(III) by air is a very slow process at the thermal water surface (McCleskey et al., 2004; Nordstrom et al., 2005). Consequently, for concentrations of H_2S >~0.5 mg/L, As is reduced (Fig. 7) and As(III) is often the dominant As species for many thermal springs (Ballantyne and Moore, 1988; Donahoe-Christiansen et al., 2004; Landrum et al., 2009; Nordstrom et al., 2005). For the spring waters collected for this study, the median As(III)/As(T) ratio was 0.87. Dilute thermal waters tend to be the most oxidized and the As(III)/As(T) ratio for most of these samples is ~ 0.5. Mixing with shallow oxygenated ground waters (Donahoe-Christiansen et al., 2004) and stagnant pools or low-flowing springs with higher water residence times may create conditions favorable for the oxidation of As(III) to As(V). In some pools, the As(III)/As(V) ratio can vary depending on proximity to the main orifice and collection depth. Microbes rapidly catalyze As(III) oxidation at the spring surface and along drainage channels once the reduced sulfur species are depleted by degassing and oxidation (D'Imperio et al., 2007; Donahoe-Christiansen et al., 2004; Langner et al., 2001; Nordstrom et al., 2005; Wilkie and Hering, 1998). We have observed rapid oxidation of As(III) along numerous thermal drainages in YPVF once H_2S concentrations decreased including in a neutral-Cl spring (Ojo Caliente in Lower Geyser Basin) (Fig. 8a) and an acid-SO_4 spring (Nymphy Creek located along the Norris-Mammoth corridor) (Fig. 8b). Ferrous-iron (Fe(II)) has also been shown to inhibit the oxidation of As(III) (McCleskey et al., 2004) and microbial oxidation of Fe(II) and As(III) has been shown to occur simultaneously in Nymphy Creek (Nordstrom et al., 2005).

While the majority of As redox determinations in YPVF waters used in this study were determined using hydride generation (Fig. 7 and 8), which does not quantify important thioarsenic species (Planer-Friedrich and Wallschläger, 2009), the data corroborate the findings of many studies (e.g., D'Imperio et al., 2007; Donahoe-Christiansen et al., 2004; Gihring et al., 2001; Langner et al., 2001). Arsenic(III) determinations by hydride generation is operationally defined and includes reduced As species (As(III)) that readily form arsine including arsenite and most likely methyl- and thio-arsenic species. While arsenite and arsenate are important As species in many thermal springs and drainages (López et al., 2012), especially when sulfide concentrations are low, thioarsenic species have been identified and are also important in many YPVF waters (Planer-Friedrich et al., 2020; Planer-Friedrich et al., 2007). Tri-, di-, and monothioarsenate were quantified in Ojo Caliente and its drainage in YPVF (Planer-Friedrich et al., 2007) as well as hot springs in China (Guo et al., 2017). The distribution of As species at Ojo Caliente was determined to be ~52% trithioarsenate, ~35% arsenite, ~15% dithioarsenate, and ~3% monothioarsenate (Planer-Friedrich et al., 2007). Thioarsenates are important forms of As in many neutral-Cl waters containing elevated sulfide concentrations (Planer-Friedrich et al., 2007) which include many neutral-Cl waters found in Upper, Midway, and Lower Geyser Basin (Fig. 3). Planer-Friedrich et al. (2020) discovered that the molar excess of sulfide compared to As concentrations is the most important predictor of thioarsenates. Thus, as sulfide decreases along drainages, thioarsenates also decrease (Planer-Friedrich et al., 2007). Irrespective of thermal water type and As species and complexes, arsenate is the primary end-product along thermal water drainages, and fluvial transport of As is controlled by As(V) geochemistry.

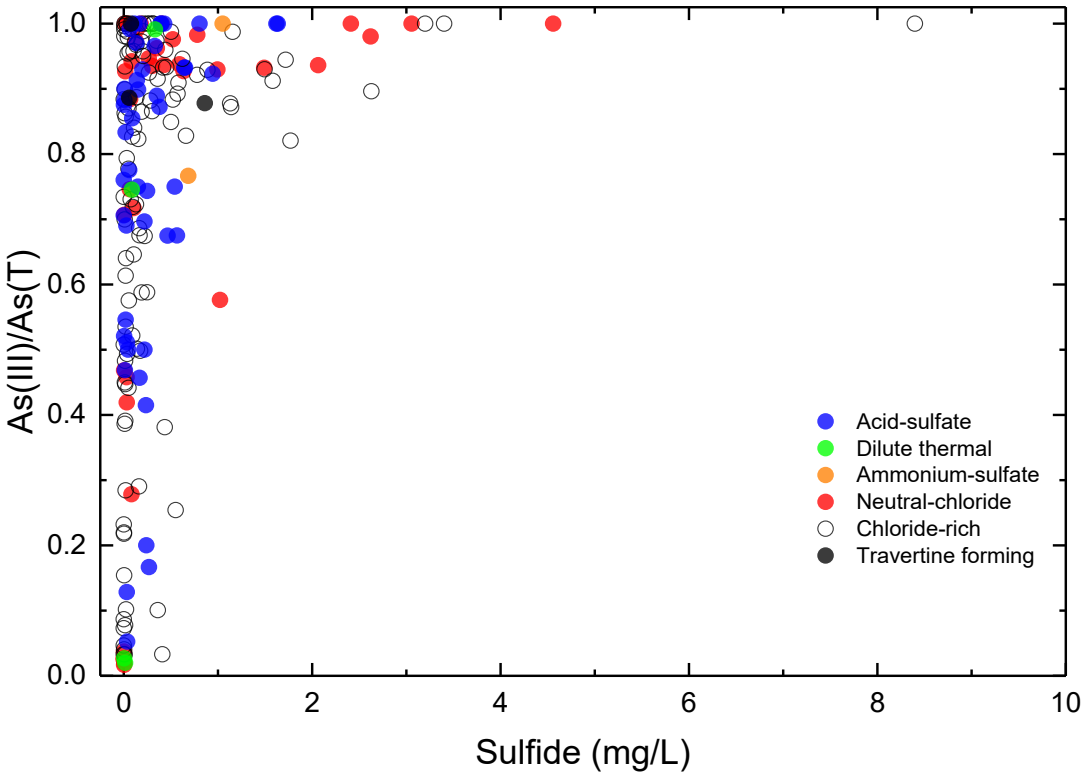

Figure 7. Dissolved As(III)/As(T) ratio relative to dissolved sulfide in Yellowstone Plateau Volcanic Field thermal waters. Data used in this figure are from Ball et al., 2010; Ball et al., 2006; Ball et al., 2002; Ball et al., 1998b; Bergfeld et al., 2019; Gemery-Hill et al., 2007; Lowenstern et al., 2012; McCleskey et al., 2005; and McCleskey et al., 2022.

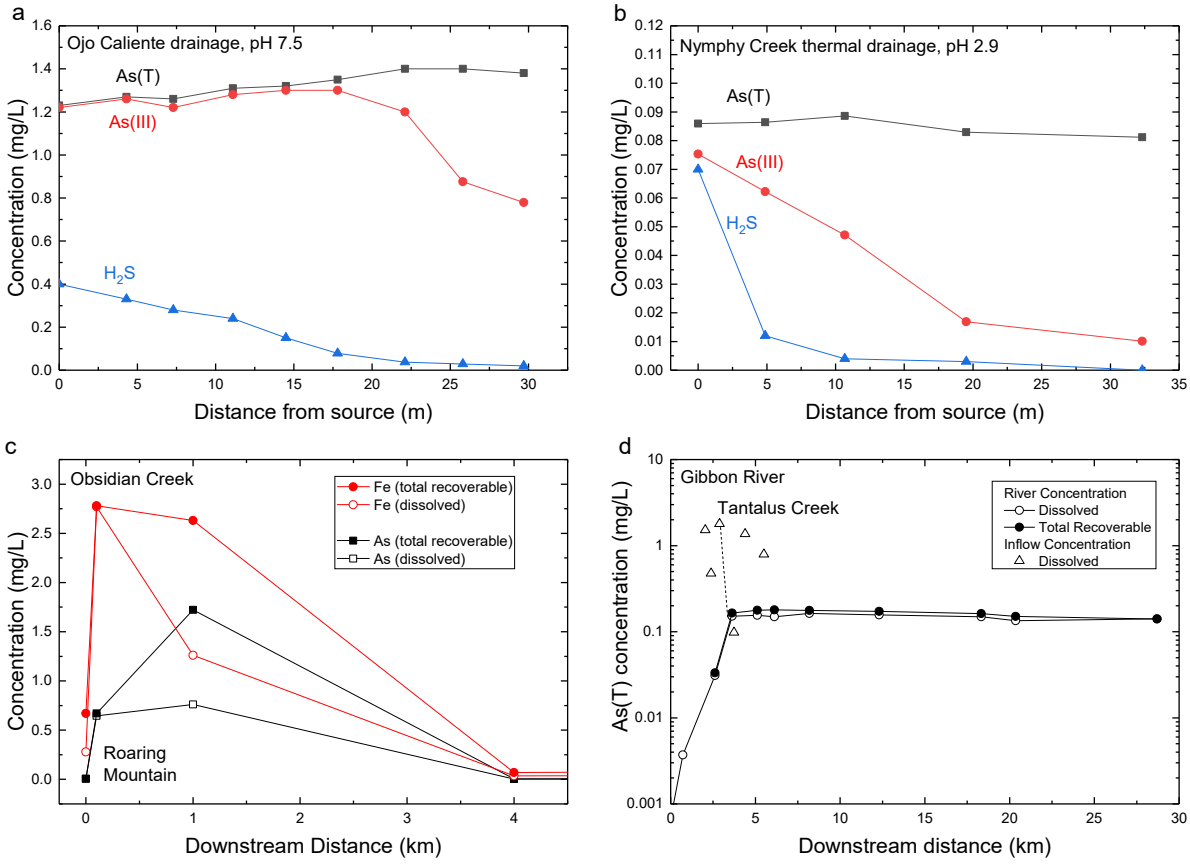

Figure 8. Plot of total dissolved As (As(T)), As(III), and H_2S concentrations along thermal drainages from Ojo Caliente in Lower Geyser Basin (a) and Nymphy Creek thermal area along the Norris-Mammoth corridor (b). Plot of As and Fe concentrations in Obsidian Creek (c) and As concentrations in the Gibbon River (d.) Total recoverable concentrations are determined in unfiltered-acidified water samples. Data used in this figure are from Ball et al., 2010; McCleskey et al., 2005; and McCleskey et al., 2022.

4.2.3 Geothermal solutes relative to arsenic

Several solutes are known to be elevated in YPVF thermal waters including alkali metals (Li, Na, K, Rb, and Cs), halogens (F, Cl, and Br), metalloids (B, SiO_2, Ge, As, and Sb), H_2S,

SO_4, Hg, W, and Mo. Many of these solutes are recognized as being a typical suite of "geothermal solutes" (Ellis and Mahon, 1977; Planer-Friedrich et al., 2020; Webster and Nordstrom, 2003). The concentrations of most geothermal solutes are positively correlated with each other, except for H_2S/SO_4 and Hg. Sulfur and Hg chemistry are complicated because they not only exist in various redox states but can also exist as gas and exsolve from solution (Sherman et al., 2009), and they form secondary minerals. Figure 9 shows As concentrations relative to B, Sb, W, and Mo.

Boron and As concentrations are positively correlated ($R^2 = 0.5$; Significance $F = 5x10^{-38}$) in the dilute thermal, neutral Cl, Cl-rich, and travertine-forming waters in the YPVF (Fig. 9a). For acid sulfate waters, B concentrations are not correlated with As concentrations (Significance $F = 0.2$). However, B is enriched relative to As in thermal springs from Washburn Hot Springs and Calcite Springs. Waters from Washburn Hot Springs are also high in NH_4 and SO_4 due to hot water flowing though oil-bearing sedimentary rocks (Fournier, 2005; Love and Good, 1970). It is thought that these thermal waters undergo a distillation process concentrating NH_3 (Fournier, 2005; Holloway et al., 2011). Since B is known to be volatile in thermal waters (Cullen et al., 2021) and since B is present in high concentrations in oil-field waters (Floquet et al., 2016), B is also concentrated in waters from Washburn Hot Springs and Calcite Springs. In the YPVF, volatile As concentrations of 0.5 to 200 mg/m^3 at the surface of hot springs have been measured and the most frequently identified species was $(CH_3)_2AsCl$ (Planer-Friedrich et al., 2006). As far as we know, neither the volatile As flux nor the fraction of the total As volatilized have been determined in the YPVF. Since B is enriched in vapor when the groundwater boils (Cullen et al., 2021; Ellis and Mahon, 1977), B tends to be enriched relative to non-volatile species in acid-SO_4 waters. Moreover, since arsenite (where H_3AsO_3 is the dominant As(III) species in most YPVF

thermal waters, determined using PHREEQCI (Parkhurst and Appelo, 1999)) behaves somewhat similar to B (where H_3BO_3 is the dominant B species) (Campbell and Nordstrom, 2014), if As readily formed volatile species in YPVF, As would also concentrate in acid-SO_4 waters. However, As concentrations are typically very low in NH_4-SO_4 rich and acid-SO_4 waters (Fig. 4a and 6b) and many acid-SO_4 samples have relatively high B/As ratios (Fig. 9a). Furthermore, arsenate is the dominant species in many acid-SO_4 waters, which is expected to be less volatile than reduced As species. Thus, we surmise that volatile As is a small component in the YPFV's As mass balance.

Antimony, W, and Mo exist as either oxyanions or thioanions, similar to As, and are also enriched in geothermal waters (Landrum et al., 2009; Planer-Friedrich et al., 2020). The average mass ratio of Sb to As is 0.04 ± 0.02 (excluding samples from Crater Hills) and apart from a few samples, Sb is positively correlated ($R^2 = 0.5$; Significance $F = 2x10^{-44}$) with As (Fig. 9b). However, the average mass ratio of Sb to As for seventeen YPVF rhyolites was 0.2 ± 0.06 (Harrison et al., 2022), suggesting incongruent dissolution of rhyolite or preferential loss of Sb from solution. The mass ratio of Sb to As in a small number of water samples from Norris Geyser Basin are the most disparate (0.001 to 0.16). Thus, Sb concentrations likely have high variability, and the fate of Sb is different than that of As in hydrothermal environments. Antimony is enriched relative to As in sinter compared to thermal waters (Churchill et al., 2021a) which may be the cause of some of the disparate Sb/As ratios. Furthermore, in El Tatio sinter, Sb was found to be enriched in geyserite precipitates whereas As was associated with ferric oxides and microbial biofilms (Landrum et al., 2009). Some thermal waters with the highest As concentrations, including waters from Crater Hills, contain relatively low concentrations of Sb, W, and Mo (Fig. 9b, c, and d). Furthermore, concentrations of Sb, W, and

Mo are relatively low in the carbonate-rich waters from Mammoth and Snake River Hot Springs. Two distinct trends appear for W in relation to As (Fig. 9c). Neutral-Cl springs (red circles) on the western side of the Yellowstone Caldera including Upper, Midway, Lower, and Shoshone Geyser Basins have elevated W to As mass ratios (0.3 ± 0.1) compared to the Cl-rich waters (orange and green circles) predominantly from Norris, Sylvan, and Gibbon Geyser Basins (0.04 ± 0.02). Finally, the average Mo to As mass ratio is 0.03 and while Mo concentrations generally increase alongside As (Fig. 9d), the correlation is comparatively lower than other geothermal solutes ($R^2 = 0.3$; Significance F = $1x10^{-18}$). The average mass ratio of Mo to As for seventeen YPVF rhyolites was 1.5 ± 0.6 (Harrison et al., 2022), suggesting incongruent dissolution of rhyolite or preferential loss of Mo from solution.

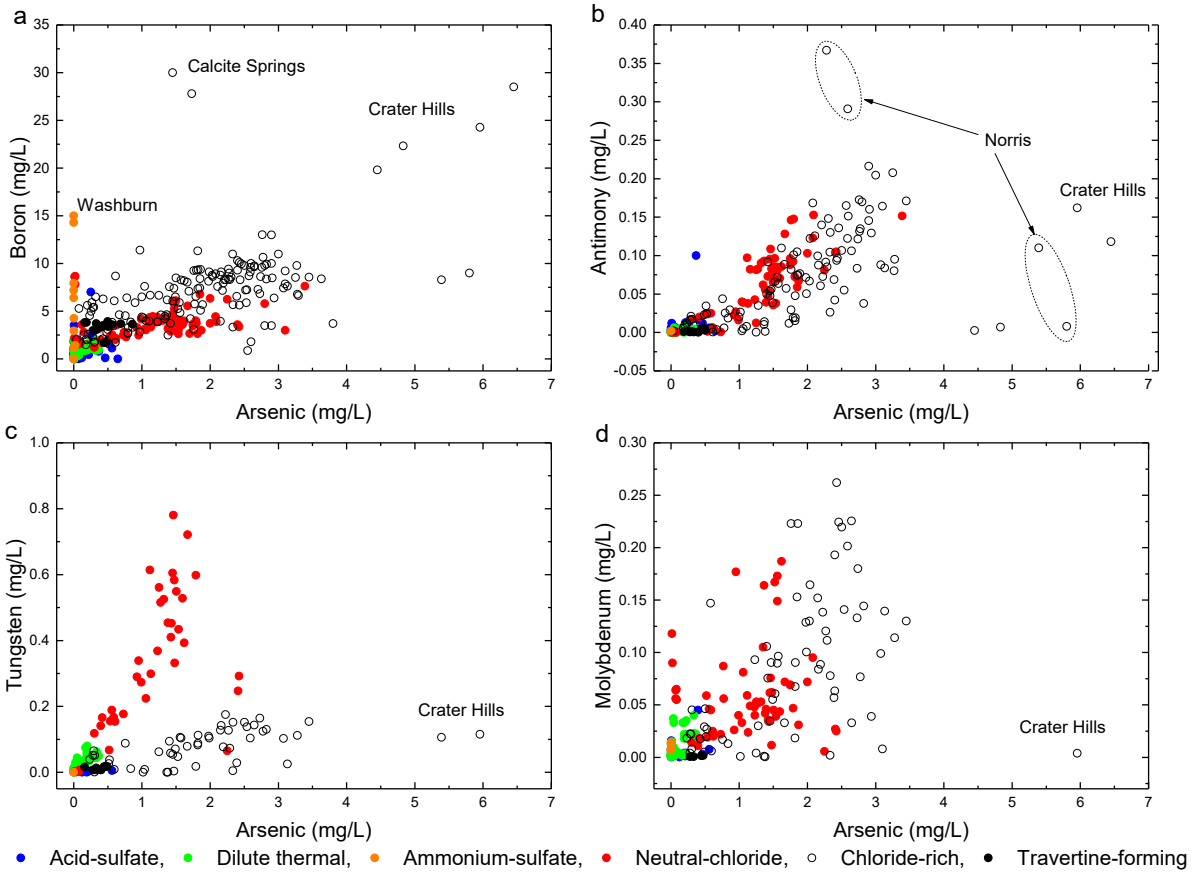

Figure 9. Plot of arsenic in relation to B (a), Sb (b), W (c), and Mo (d) in thermal waters sampled form the Yellowstone Plateau Volcanic Field. Data used in this figure are from McCleskey et al., 2022.

4.2.4 Microbiological processes

Chemolithotrophic microorganisms, or organisms that generate energy (-trophic) from inorganic (-litho-) forms of chemical (chemo-) energy are known to rapidly oxidize As(III) to As(V) in YPVF hot springs (D'Imperio et al., 2007; Donahoe-Christiansen et al., 2004; Gihring et al., 2001; Langner et al., 2001). In an acid-SO_4 hot spring (pH 3.1, 58 to 62°C) located in Norris Geyser Basin, transformation of As(III) to As(V) rapidly occurred along the hot spring outflow channel but only after hydrogen sulfide (H_2S) concentrations fell to below 0.2 mg/L (Langner et al., 2001). In thermophilic and hyperthermophilic microorganisms, the oxidation of As(III) is catalyzed by one of several enzymes including arsenite oxidase (Aio) and anaerobic arsenite oxidase (Arx) (Hamamura et al., 2009; Inskeep et al., 2007; Jiang et al., 2014). In one study, homologs of Aio were identified among diverse thermophilic bacteria inhabiting hot springs across numerous geyser basins in the YPVF, including springs that span temperatures from 74°C to 90°C and pH from 2.6 to 8.0 (Hamamura et al., 2009). Total As concentrations in these springs ranged from 0.2 to 10 mg/L. Further, the kinetics of biotic As(III) oxidation were faster in low pH springs, although As(III) oxidation was still detectable in springs with neutral to alkaline pH. The lower rates of As(III) oxidation in the neutral to alkaline pH springs was attributed to the presence of higher concentrations of bisulfide (HS^-; pKa = ~ 6.4 at 80°C (Amend and Shock, 2001), a potent scavenger of oxygen that is the presumed oxidant coupling with As(III) oxidation. Sequencing of genes encoding Aio from these communities identified

several genera within the bacterial order Aquificales as the most likely populations involved in As(III) oxidation in these springs including populations closely related to *Hydrogenobaculum* in acidic springs and *Sulfurihydrogenium* and *Thermocrinis* in circumneutral to basic springs (Hamamura et al., 2009). These findings are consistent with cultivation studies showing that members of these genera, including strains of *Hydrogenobaculum* and *Thermocrinis* isolated from springs in the YPVF, can oxidize As(III) (Donahoe-Christiansen et al., 2004; Härtig et al., 2014). In addition to Aquificales, Hamamura et al. (2009) identified Aio protein homologs affiliated with members of the Deinococci, specifically those related to *Thermus*, in addition to several Proteobacteria. Several *Thermus* strains with the ability to oxidize As(III) have been isolated from neutral-Cl hot springs in Lower Geyser Basin and these have been linked to high As(III) oxidation rates in several of these springs (Gihring et al., 2001). Similarly, the proteobacterium *Acidicaldus*, isolated from an acid Cl-SO_4 rich hot spring in Norris Geyser Basin where As(III) oxidation had been demonstrated (Langner et al., 2001), was shown to catalyze As(III) oxidation but only in the absence of H_2S (D'Imperio et al., 2007). That heterotrophic growth of this strain was insensitive to H_2S suggests that Aio or other components of As(III)-dependent chemolithoautotrophic growth may be inhibited by H_2S and its oxidation intermediates.

To examine the distribution and diversity of chemotrophic microorganisms putatively involved in As(III) oxidation and As(V) reduction across the YPVF, including potential microbial taxa that may have been overlooked in previous studies, 32 community metagenomes previously compiled from chemosynthetic hot springs (Colman et al., 2020) were examined for homologs of Aio and Arx proteins. Homologs were classified taxonomically at various taxonomic ranks based on their sequence homology to proteins from known organisms, as

determined by BLASTp analyses (Altschul et al., 1990). The taxonomic composition of protein homologs identified in this study are reported in Supplementary Table S1. The "relative abundance" of protein homologs within a community was also determined by read mapping. More specifically, protein encoding genes were scaled to the summed reads per kilobase pair per million mapped read (RPKM) values for all genes within a spring, allowing for a comparison of the relative abundances of homologs (and the organisms whose genomes encode them) across pH and temperature gradients. The taxonomic composition of the homologs was then examined across three broad pH realms (pH <5.0, pH 5.0 to 7.0, and pH >7.0), corresponding to those that have previously been shown to largely demarcate chemosynthetic microbial diversity in the YPFV (Colman et al., 2016; Colman et al., 2019; Inskeep et al., 2013; Takacs-vesbach et al., 2013).

Homologs of As(III) oxidases (Aio and Arx proteins) were identified in 18 of the 32 communities examined and these spanned a pH range from 1.6 to 9.0 and a temperature spanning 62°C to 91°C (Fig. 10), encompassing nearly the entire range of pH and temperature space that support chemosynthetic microbial communities in the YPVF (Colman et al., 2019; Inskeep et al., 2013). The distribution of Aio and Arx homologs was more limited in communities inhabiting acidic or moderately acidic springs (pH <7.0; homologs identified in 12/26 springs) when compared to those inhabiting circumneutral to basic springs (pH >7.0; homologs identified in 7/7 springs). This observation is consistent with the lower concentrations of As in fluids sourcing acid-SO_4 springs. In microbial communities inhabiting acidic springs (pH <3.0), the majority of homologs were affiliated with the archaeal order Sulfolobales and, in several cases, their host organisms represented a large fraction of the microbial community. These organisms were largely associated with the genera *Acidianus* and *Stygiolobus*, the latter of which has yet to be

cultivated out of a hot spring in the YPVF. The sole cultivar of *Stygiolobus* from the Azores geothermal field in Portugal was not tested for its ability to oxidize As(III) (Segerer et al., 1991). However, a strain of *Sulfolobus acidocaldarius* (order Sulfolobales), which is a close relative of *Stygiolobus*, has been shown to oxidize arsenite and couple this to cell growth in pure culture studies (Sehlin and Lindström, 1992). Moreover, *Acidianus* cultures have been previously shown to oxidize As(III) (Tec-Caamal et al., 2019). In addition to Sulfolobales, several bacterial populations affiliated with *Hydrogenobaculum* (order Aquificales) were identified with the potential for As(III) oxidation, which is consistent with previous studies showing this capability in this genus (Donahoe-Christiansen et al., 2004). In microbial communities inhabiting moderately acidic springs (pH 5.0 to 7.0), the predominant organisms with the putative capability to oxidize As(III) were affiliated with *Thermocrinis* and *Thermus*, consistent with the previously demonstrated As(III) capability in these bacterial genera (Gihring et al., 2001; Härtig et al., 2014). In addition, homologs of As(III) oxidizing enzymes (AioA) were identified that were taxonomically most closely related to *Pyrobaculum* (Archaea) and Chloroflexi (Bacteria). The presence of AioA encoded in *Pyrobaculum* genomes (and the consequent putative capacity to oxidize As(III)) has been documented for some *Pyrobaculum* strains, including genomes recovered from the YPVF (Jay et al., 2016). To the authors' knowledge, As(III) oxidation activity or the genetic potential for As(III) oxidation in Chloroflexi has yet to be reported in the YPVF, although Aio genes affiliated with Chloroflexi have been reported in the El Tatio geothermal field in Chile (Summers Engel et al., 2013). In circumneutral to basic springs (pH >7.0), the predominant putative As(III) oxidizing organisms were affiliated with *Thermocrinis*, *Thermus*, *Pyrobaculum*, and Caldarchaeales (formerly Aigarchaeota). Members of the

Caldarchaeales have yet to be cultivated (from the YPVF or other geothermal fields) and it is therefore unclear whether these organisms can oxidize As(III).

Chemotrophic microorganisms are also known to reduce As(V) to As(III) (Oremland and Stolz, 2000; Stolz and Oremland, 1999; Zhou et al., 2018), in particular members of the archaeal genus *Pyrobaculum* (Huber et al., 2000) and the bacterial genus *Thermus* (Gihring and Banfield, 2001), although far fewer studies have focused on how microorganisms influence this redox transformation in the YPVF relative to As(III) oxidation. In microorganisms, dissimilatory As(V) reduction is driven by the enzyme arsenate reductase (ArrA) (Danczak et al., 2019). In addition, several enzymes related to ArrA (within the dimethyl sulfoxide-molybdopterin (DMSO-M) family and termed ArrA-like herein) have been suggested to also be involved in As(V) reduction in several archaeal strains, including *Pyrobaculum* (Cozen et al., 2009; Huber et al., 2000). In one such study in the YPVF, a *Pyrobaculum* strain was isolated from a high As (10 mg/L), sulfidic (0.7 mg/L HS^-/H_2S), and slightly acidic hot spring (pH 6.1; 78°C) from Joseph's Coat Hot Springs and shown to be capable of reducing As(V) to As(III) (Jay et al., 2015). When grown in the presence of elemental sulfur and As(V), the organism was shown to produce a variety of thioarsenate species. During growth, As(III) generated by As(V) reduction is thought to react with elemental sulfur, resulting in the formation of thioarsenate compounds. Thioarsenates have been shown to support the metabolism of *Thermocrinis* (Härtig et al., 2014), which is a common co-inhabitant with *Pyrobaculum* in circumneutral to basic springs in the YPVF (Colman et al., 2016; Inskeep et al., 2013). In another cultivation study, several bacterial *Thermus* strains were shown to catalyze As(V) reduction under anaerobic conditions (Gihring and Banfield, 2001). Both *Pyrobaculum* and *Thermus* are common components of communities inhabiting circumneutral to neutral-Cl hot springs in the YPVF that are sourced by the parent

hydrothermal aquifer (Colman et al., 2016; Inskeep et al., 2013). However, far less is known of organisms potentially involved in As(V) reduction in moderately acidic to acidic springs in the YPVF.

To examine the distribution of organisms putatively capable of As(V) reduction in the YPVF, including those inhabiting acidic springs, the same approach described above was used to examine the 32 community metagenomes for homologs of ArrA and ArrA-like proteins. ArrA-like homologs were identified based on phylogenetic placement within a clade previously implicated in As(V) reduction in *Pyrobaculum arsenaticum* (locus tag Pars_0389) (Cozen et al., 2009). Organisms putatively capable of As(V) reduction were identified in 25 of the 32 hot spring communities examined and these spanned a pH range from 1.6 to 9.0 and a temperature spanning 62°C to 91°C (Fig. 10). As such, the ability to reduce As(V) in chemosynthetic communities in YPVF springs appears to be more widespread than the ability to oxidize As(III). This may point to these communities being oxidant limited, as has been previously suggested (Shock et al., 2010), while also alluding to the potential importance of As(V) as an oxidant capable of sustaining thermophilic microorganisms. ArrA or ArrA-like homologs were identified in 13 of the 20 communities from acidic springs (pH <5.0) and these were primarily affiliated with members of the archaeal order Sulfolobales, the archaeal genus *Thermoproteus,* and the bacterium *Hydrogenobaculum*. A previous study documented As(V) reduction in a culture of *S. acidocaldarius* (order Sulfolobales), although it is not clear that this is coupled to growth. Rather, evidence indicates that As(V) reduction is attributed to a soluble metabolite released during growth (Mikael Sehlin and Börje Lindström, 1992). The authors are unaware of definitive evidence showing that *Hydrogenobaculum* or *Thermoproteus* can catalyze As(V) reduction. ArrA or ArrA-like homologs were identified in all six of the moderately acidic springs (pH 5.0 to

7.0) surveyed and these corresponded to a diverse array of taxa including those affiliated with the bacterial lineages Chloroflexi, Chlorobi, and *Thermus* and the archaeal lineages *Thermoproteus* and *Pyrobaculum*. The majority of the Chloroflexi and Chlorobi ArrA-like homologs were only distantly related to those from characterized cultures, as well as proteins encoded by genomes recovered from other hot spring environments. It is thus unclear if members of the Chloroflexi or Chlorobi can respire As(V), although it is worth noting that ArrA homologs have been detected in members of these lineages previously (Yamamura and Amachi, 2014). The detection of ArrA or ArrA-like homologs in *Thermus* and *Pyrobaculum* in YPVF hot spring communities is consistent with the demonstrated ability of cultivars from such communities to reduce As(V) (Gihring et al., 2001; Jay et al., 2015). Like communities inhabiting moderately acidic springs, those inhabiting circumneutral to basic springs (pH >7.0) universally included members that encoded homologs of ArrA and ArrA-like proteins. These were primarily affiliated with the archaeal lineage *Pyrobaculum* and the bacterial lineages, Chlorobi and Chloroflexi.

The collective observations presented here point to the key role that microorganisms play in the transformation and thus toxicity and mobility of As compounds in hot springs of the YPVF. Further, they identify gaps in our understanding of As biogeochemistry, including the role of microorganisms in As(III) oxidation and As(V) reduction in springs with pH <5.0. The potential role of several newly identified microbial taxa involved in As transformations need to be examined, including those of various members in As(III) oxidation such as members of the Sulfolobales, Caldarchaeales, and *Pyrobaculum*. Likewise, several microbial groups may have thus far been overlooked for their role in As(V) reduction, including members of the Sulfolobales, *Thermoproteus*, *Hydrogenobaculum*, Chlorobi, and Chloroflexi. Bridging these knowledge gaps could provide a more holistic picture of As biogeochemical cycling in the YPVF

and yield new insights into the key processes that support and maintain biodiversity in this unique environmental setting.

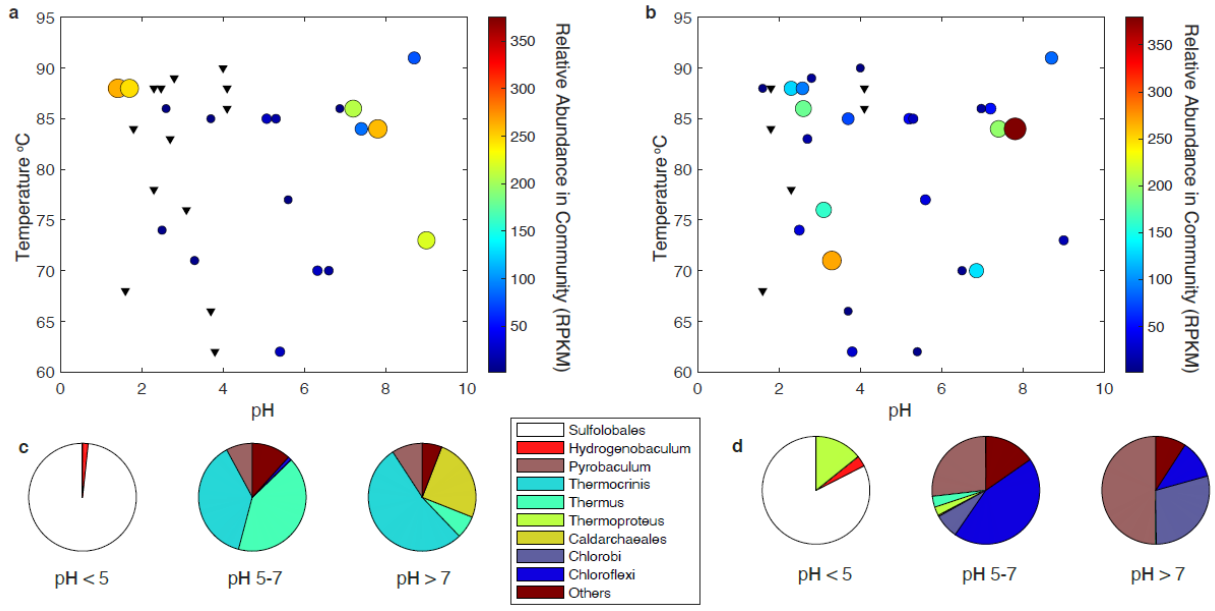

Figure 10. A plot showing the distribution and relative abundances of arsenite oxidase and arsenate reductase-like proteins among communities inhabiting high-temperature hot springs in the Yellowstone Plateau Volcanic Field (YPVF). Scatter plots are shown for the presence (circles) or absence (down-facing triangles) of (a) arsenite oxidase large subunit (AioA, ArxA) and (b) arsenate reductase large subunit (ArrA, ArrA-like) encoding genes among 32 spring communities, as arrayed by spring temperature and pH. Gene presence was identified based on phylogenetic affiliation with previously identified AioA, ArrA, and ArxA from isolates (Danczak et al., 2019; Zargar et al., 2012) and the presumed arsenate respiring ArrA-like subunit of *Pyrobaculum arsenaticum* (Pars_0389; Cozen et al., 2009) that is distantly related to other ArrA. Gene presence is scaled to the summed reads per kilobase pair per million mapped read

(RPKM) values for all genes within a spring. RPKM values for each gene on a contig were calculated by the number of mapped reads to contig / (contig length/1,000 x total reads in the metagenome / 1,000,000). The RPKM expression thus quantifies the “relative abundance” of a gene within a particular spring community metagenome and springs are colored based on the RPKM abundance scale to the right of the scatterplots. The taxonomic distribution of arsenite oxidase (c) and arsenate reductase (d) genes are shown below the scatter plots and are binned according to the three major pH realms that demarcate biodiversity in YPVF. Taxonomic designations were made based on BLASTp searches (Altschul et al., 1990) of encoded proteins against the NCBI database (Sayers et al., 2022).

5. Fate of geothermal arsenic in rivers

Most of the water discharged from YPVF thermal springs ultimately ends up in nearby rivers and monitoring the chemistry of the major rivers draining the YPVF is a way to capture and integrate the thermal and chemical contribution from the entire field (Fournier, 1989; Friedman and Norton, 1990; Hurwitz et al., 2007; McCleskey et al., 2019b). The overall fluvial As concentrations and fluxes in YPFV (Fig. 11 and Table 1) have been quantified as a result of this extensive river monitoring program and of multiple synoptic studies in many of the rivers (McCleskey et al., 2012; McCleskey et al., 2016; McCleskey et al., 2010; McCleskey et al., 2019a; McCleskey et al., 2019b).

Fluvial transport of As in YPVF is large because of the elevated As concentrations in many thermal waters discharging into rivers and very little As is attenuated in drainages, creeks, and rivers. Fluvial transport of As in the Gibbon River (Fig. 8d) is like most other major rivers in the YPVF (e.g., Firehole, Madison, Snake, Fall, Yellowstone, and Gardner Rivers) because the total dissolved As concentration is similar to the total recoverable As concentration and only a minimal amount (<5%) of As is attenuated from primary sources to the park boundary (McCleskey et al., 2012; McCleskey et al., 2020; McCleskey et al., 2016; McCleskey et al., 2019b). The low attenuation of As is due to low particulate Fe concentrations, little iron-rich sediment, circumneutral pH, and silica coatings on sediments resulting in decreased sorption capacity (McCleskey et al., 2010; Nimick et al., 1998). Furthermore, As transport in the YPVF is partly dependent on As(V) sorption because As is oxidized along drainages (e.g., Fig. 8a and 8b). Adsorption of As(V) by Fe oxides reaches a maximum at pH 3 to 4, and gradually decreases as pH increases (Hingston et al., 1971). The only stream reach in the YPVF where we have observed extensive attenuation of As is in the upper reach of Obsidian Creek. In this acidic (pH

3) stream reach, As decreases where the particulate Fe increases, suggesting sorption onto Fe oxide precipitates and settling onto the streambed (Fig. 8c). The river reach is also rich in organic matter which has been shown to sorb and co-precipitate As (López et al., 2012).

The current monitoring network provides information at several scales (Yellowstone wide, watersheds, and individual geyser basins). The Madison, Yellowstone, Snake, and Fall River monitoring sites capture the hydrothermal discharge within their watersheds, and the sum of these four rivers captures the entire hydrothermal discharge from Yellowstone National Park. Additional monitoring sites along their tributaries provide higher resolution and can be used to capture the As flux at geyser basin scales. The total As flux from Yellowstone is 183 ± 10 metric ton/yr (Table 1). The As flux from the Madison River (110 metric tons/year or 60.1% of the total flux) is the largest of the four main rivers draining YPVF followed by the Yellowstone River (50 metric tons/year or 27.3%), the Snake River (15 metric tons/year or 8.2%), and the Fall River (8 metric tons/year or 4.4%). While the As flux from YPVF is vast, it may further increase with anomalous volcanic activity. For example, a two-fold increase in As output at Lassen occurred during volcanic unrest in 2015 (Ingebritsen and Evans, 2019). Thus, knowledge of the major As source locations and background As fluxes is important for managing downstream water resources should volcanic unrest occur. The combined thermal springs along the Firehole River (Upper, Midway, and Lower Geyser Basins) are the largest source of As where nearly 86 metric ton/yr of As are discharged which accounts for nearly 47% of the As flux from the YPVF. Other large As sources include springs in and around Yellowstone Lake (20 metric ton/yr of As, 11% of the total As flux); discharge from Norris Geyser Basin as measured at Tantalus Creek (7.2 metric ton/yr of As, 4.0% of the total As flux); and one single feature, the Boiling River,

discharges 9.2 ± 0.9 metric ton/yr of As which accounts for 4.9 % of the total As flux from YPVF (Fig. 11, Table 1).

In addition to the As mass flux, river As concentrations are also significant. The occurrence of elevated As concentrations in river waters within and downstream from YPVF has been a long-term concern of water managers. Cities downstream from and villages within YPVF must provide treatment for As. For example, ferric chloride ($FeCl_3$) treatment is used to limit As in drinking water at Old Faithful whose source is the upper Firehole River (National Park Service, 2020). Additionally, alluvial aquifers recharged by YPVF rivers contain elevated As concentrations (Montana Department of Environmental Quality, 1995; Nimick et al., 1998). Furthermore, rivers in Yellowstone are widely used for recreational purposes including swimming, fishing, and drinking supplies for many backcountry campers. Some of the most popular river "swim holes" in YPVF occur downstream of thermal sources where river waters are warm and As concentrations are elevated (>10 ppb). Thus, it is prudent to know typical low-flow fluvial As concentrations (July to October), which is the time of year when river As concentrations are elevated and the number of visitors is highest. During low-flow conditions, As concentrations exceed the EPA standard for drinking water of 10 µg/L for long reaches along the Madison River, Firehole River, Gibbon River, Yellowstone River, Snake River, Lewis River, Fall River, and Boundary Creek (Fig. 11 and Table 1). In addition, As concentrations in short reaches of the Bechler River and Obsidian Creek exceed 10 µg/L. During low-flow conditions, As concentrations finally fall below the 10 µg/L maximum contaminant level (MCL) approximately 700 river km downstream from the park boundary along the Madison-Missouri Rivers and approximately 350 river km downstream from the park boundary along the Yellowstone River.

Fluvial transport of As downstream from thermal sources in YPVF is largely conservative and large compared to most other rivers receiving geothermal As. For example, the As flux in the Jemez River, Valles Caldera, NM, decreases by nearly 95% within about 20 km of the main As source (Reid et al., 2003) and in Mill Creek, Lassen, CA, As decreases as much as 80% within about 75 km. While fluvial As transport from the YPVF is large (183 ± 10 metric ton/yr, Table 1), the As transport from El Tatio, Chile is even larger (about 500 metric ton/yr; Ingebritsen and Evans, 2019).

.

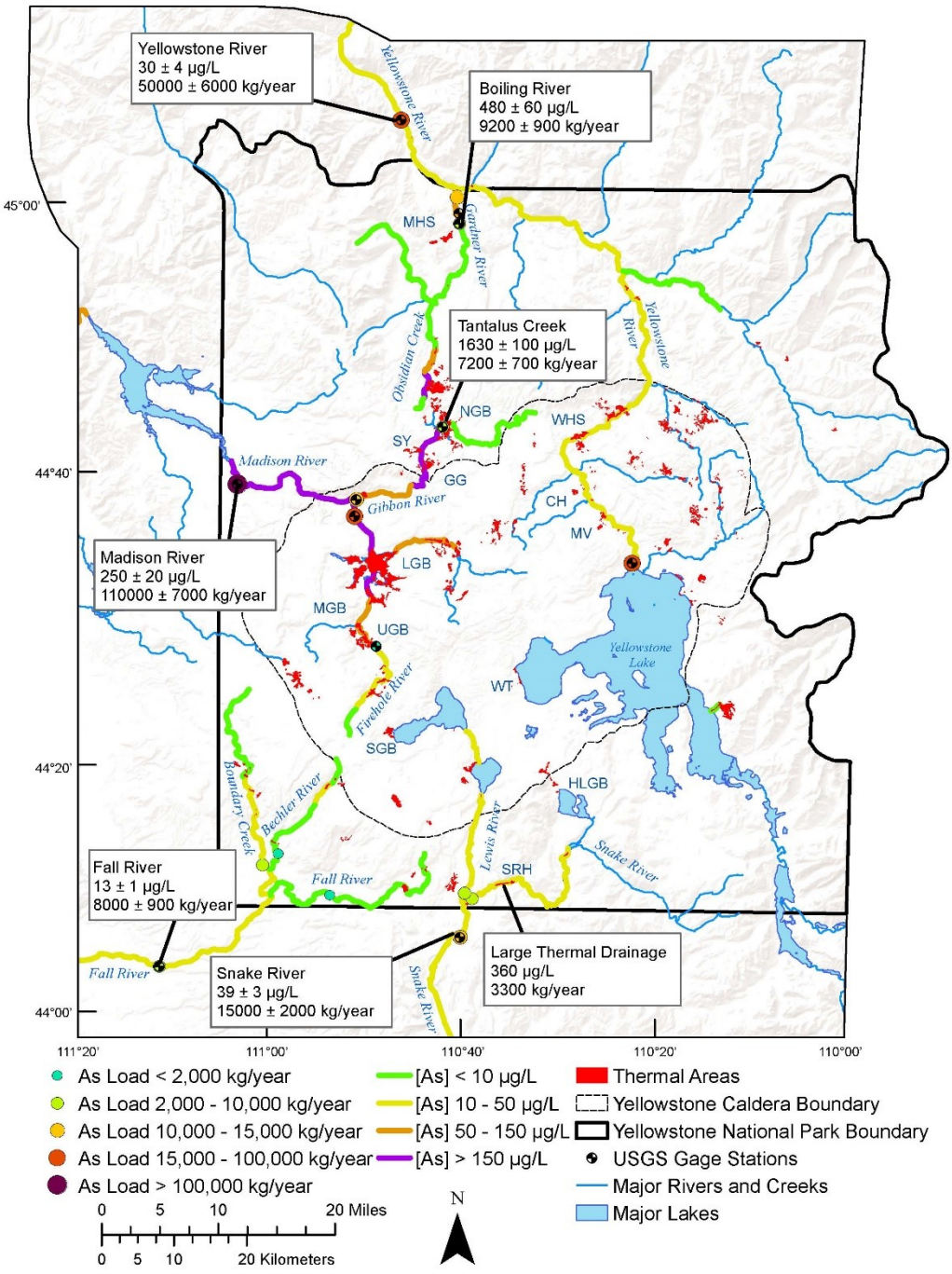

Figure 11. River water arsenic concentrations and loads in the Yellowstone Plateau Volcanic Field represented by colored lines and dots. The Yellowstone Caldera and thermal area boundaries are adapted from Vaughan et al. (2013). Data used in this figure are from McCleskey et al., 2017; McCleskey et al., 2022; and McCleskey et al., 2019c.

Table 1. Annual arsenic flux and the percentage of arsenic exiting the Yellowstone Plateau Volcanic Field from the four major watersheds and subwatersheds draining thermal waters, arsenic concentrations determined during low-flow (September) conditions, and specific conductance proxy parameters used to determine fluvial arsenic concentration (McCleskey et al., 2012; McCleskey et al., 2020; McCleskey et al., 2016; McCleskey et al., 2019b).

River Site[A]	Annual As Flux[C] (metric ton/yr)	As exiting YPVF (%)	As concentration[D] (µg/L)	Proxy Parameters[E] a	b	R^2
Madison River near western boundary[B]	**110 ± 7**	60.1	250 ± 20	0.618	-8.49	0.97
Firehole River above confluence with Gibbon R.[B]	**86 ± 3**	47	380 ± 30	0.768	-16.4	0.98
Firehole River upstream from Old Faithful[B]	**2.0 ± 0.1**	1.1	41 ± 6	0.34	-1	0.81
Gibbon River above confluence with Firehole R.[B]	**14 ± 2**	7.7	140 ± 10	0.306	13.5	0.94
Tantalus Creek[B]	*7.2 ± 0.7*	3.8	1630 ± 100	---	---	---
Yellowstone at Corwin Springs[B]	**50 ± 6**	27.3	30 ± 4	0.167	-7.59	0.98
Yellowstone Lake outflow[B]	*20 ± 2*	10.9	16 ± 1	---	---	---
Gardner River below Boiling River[B]	**11 ± 1**	6.0	105 ± 20	0.220	-30	0.94
Boiling River	*9.2 ± 0.9*	4.9	480 ± 60	---	---	---
Fall River below Bechler River[B]	**8.0 ± 0.9**	4.4	13 ± 1	0.110	-2.4	0.97
Bechler River above Boundary Creek	*1.8 ± 0.2*	1.1	8 ± 1	---	---	---
Boundary Creek above Bechler River	*4.5 ± 0.5*	2.7	50 ± 6	---	---	---
Fall River above Bechler River	*1.6 ± 0.2*	1.1	9 ± 1	---	---	---
Snake River below Lewis River[B]	**15 ± 2**	8.2	39 ± 3	0.149	-6.2	0.96
Snake River above Lewis River	*6.7 ± 0.7*	3.8	45 ± 4	---	---	---
Large thermal drainage at Boundary Trail Bridge	*3.3 ± 0.3*	1.8	360 ± 30	---	---	---
Lewis River above Snake River	*8.2 ± 0.8*	4.4	38 ± 3	---	---	---
Lewis Lake outflow	*2.9 ± 0.3*	1.6	25 ± 2	---	---	---
Shoshone Lake outflow	*2.4 ± 0.3*	1.3	24 ± 2	---	---	---
Total YPVF	183 ± 10					

[A] Subwatersheds are identified by increasing indentation

[B] Gage site shown on Fig. 11

[C] Determined using continuous SC proxy except for values in italics which were determined from low-flow synoptic studies

[D] Typical low-flow concentration measured in September

[E] As (µg/L) = a SC + b, where SC is specific conductance in µS/cm (equation 1)

6. Conclusions

This study on As biogeochemistry in the YPVF hydrothermal system provides insights on As sources, important processes controlling As concentrations, speciation, transformations, and fluvial transport that are expected to be important in other volcanic and hydrothermal settings. Major conclusions drawn from this study are:

- Arsenic concentrations in YPVF thermal waters vary depending on the thermal water type. Springs with low As concentrations include acid-SO_4 (0.1 ± 0.1 mg/L), NH_4-SO_4 (0.003 ± 0.007 mg/L), and dilute thermal waters (0.1 ± 0.1 mg/L); travertine-forming waters have moderate As concentrations (0.4 ± 0.2 mg/L); and neutral-Cl waters (1.2 ± 0.8 mg/L) common in the western portion of the Yellowstone Caldera and Cl-rich waters (1.9 ± 1.2 mg/L) primarily from Basins near the Caldera boundary have elevated As concentrations.
- Arsenic in YPVF hot springs is mostly derived from high temperature (≥ 275 °C) leaching of rhyolites.
- There are several processes in YPVF that impact As concentrations, including decompressional boiling that results in evaporative concentration of As in the remaining fluids and mixing of thermal waters that results in fluctuating As concentrations in many springs.
- Arsenic does not appear to be volatilized in YPFV thermal fluids and consequently vapor dominated springs (acid-SO_4 and NH_4-SO_4 waters) contain low As concentrations.
- Arsenite is often the dominant As species in thermal surface water sources and thioarsenates can also predominate in neutral-Cl waters having elevated sulfide

concentrations. Arsenate is the dominant As along drainages once the sulfide concentrations decrease due to degassing and oxidation.

- Microorganisms can catalyze the dissimilatory oxidation of arsenite or reduction of arsenate. Metagenomics analyses of hot spring communities indicate that these microbial populations are diverse and widespread in high temperature hot springs in the YPVF, suggesting a key role for microbial activity in affecting the speciation, solubility, and mobility of As in this ecosystem.
    - Microorganisms that encode the ability to oxidize arsenite include members of the bacterial order Aquificales (*Hydrogenobaculum*, *Sulfurihydrogenibium*, *Thermocrinis*), the bacterial genus *Thermus*, the archaeal order Sulfolobales (*Stygiolobus*, *Acidianus*) and members of the uncultivated archaeal order Caldarchaeales.
    - The distribution of organisms that can oxidize arsenite was more limited in acidic springs than circumneutral to basic springs, consistent with the latter spring type being enriched in arsenite relative to the former spring type.
    - Organisms that can reduce arsenate were more widespread than those that can oxidize arsenite, suggesting the importance of arsenate as an oxidant or electron acceptor capable of supporting microbial life.
    - A diversity of organisms was identified with the potential capability of arsenate reduction, including genera known to catalyze this activity (*Thermus*, *Pyrobaculum*) and several groups of organisms where this activity has yet to be demonstrated (*Sulfolobales*, *Thermoproteus*, *Hydrogenobaculum*, Chloroflexi, and Chlorobi), suggesting a need for further study of these organisms.

- The total As flux from Yellowstone rivers is 183 ± 10 metric ton/yr, with the majority of the flux being from the Madison (60.1%) and Yellowstone (27.3%) Rivers. Most of the water discharged from YPVF thermal springs ultimately ends up in a nearby river and downstream transport is extensive because As primarily exists as arsenate, low Fe concentrations in the water column and sediments, circumneutral pH, and silica coatings on sediments resulting in decreased As sorption capacity.
- Fluvial As concentrations exceed 10 µg/L (drinking water standard) in most river reaches receiving thermal water inflow.

Acknowledgements

Support was provided by the U.S. Geological Survey (USGS) Volcano Hazards Program and its Yellowstone Volcano Observatory, the USGS Water Mission Area, and the National Park Service. DRC and ESB acknowledge support from the National Science Foundation (EAR-1820658) and the NASA Established Program to Stimulate Competitive Research (EPSCoR) program (MT-19-EPSCoR-0020).

We thank the staff of Yellowstone National Park, including most recently Jeff Hungerford, Erin White, and Annie Carlson for their assistance on numerous occasions. We also thank our colleagues at the USGS including Jim Ball, Kate Campbell, JoAnn Holloway, Randall Chiu, and Paul Bliznik for the assistance in the field and laboratory.

Any use of trade, firm, or product names is for descriptive purposes only and does not imply endorsement by the U.S. Government.

Conflict of Interest: The authors declare no competing interests.

Data Availability

Data are available from online U.S. Geological Survey databases (Harrison et al., 2022; McCleskey et al., 2019a; McCleskey et al., 2022; McCleskey et al., 2019c).

References

Aiuppa, A., Avino, R., Brusca, L., Caliro, S., Chiodini, G., D'Alessandro, W., Favara, R., Federico, C., Ginevra, W., Inguaggiato, S., Longo, M., Pecoraino, G. and Valenza, M., 2006. Mineral control of arsenic content in thermal waters from volcano-hosted hydrothermal systems: Insights from island of Ischia and Phlegrean Fields (Campanian Volcanic Province, Italy). Chemical Geology, 229(4): 313-330.

Aiuppa, A., D'Alessandro, W., Federico, C., Palumbo, B. and Valenza, M., 2003. The aquatic geochemistry of arsenic in volcanic groundwaters from southern Italy. Applied Geochemistry, 18(9): 1283-1296.

Allen, E.T. and Day, A.L., 1935. Hot springs of the Yellowstone National Park. Carnegie Institution of Washington - Publication 466, Washington D.C.

Altschul, S.F., Gish, W., Miller, W., Myers, E.W. and Lipman, D.J., 1990. Basic local alignment search tool. J Mol Biol, 215(3): 403-10.

Amend, J.P. and Shock, E.L., 2001. Energetics of overall metabolic reactions of thermophilic and hyperthermophilic Archaea and Bacteria. FEMS Microbiology Reviews, 25(2): 175-243.

Ball, J.W., McCleskey, R.B. and Nordstrom, D.K., 2010. Water-chemistry data for selected springs, geysers, and streams in Yellowstone National Park, Wyoming, 2006-2008. U.S. Geological Survey Open-File Report 2010-1192.

Ball, J.W., McCleskey, R.B., Nordstrom, D.K. and Holloway, J.M., 2006. Water-chemistry data for selected springs, geysers, and streams in Yellowstone National Park, Wyoming, 2003-2005. U.S. Geological Survey Open-File Report 2006-1339.

Ball, J.W., McCleskey, R.B., Nordstrom, D.K., Holloway, J.M. and Verplanck, P.L., 2002. Water-chemistry data for selected springs, geysers, and streams in Yellowstone National Park, Wyoming, 1999-2000. U.S. Geological Survey Open-File Report 02-382.

Ball, J.W., Nordstrom, D.K., Cunningham, K.M., Schoonen, M.A.A., Xu, Y. and DeMonge, J.M., 1998a. Water-chemistry and on-site sulfur-speciation data for selected springs in Yellowstone National Park, Wyoming, 1994-1995. U.S. Geological Survey Open-File Report 98-574.

Ball, J.W., Nordstrom, D.K., Jenne, E.A. and Vivit, D.V., 1998b. Chemical analyses of hot springs, pools, geysers, and surface waters from Yellowstone National Park, Wyoming, and vicinity, 1974-1975. U.S. Geological Survey Open-File Report 98-182.

Ballantyne, J.M. and Moore, J.N., 1988. Arsenic geochemistry in geothermal systems. Geochimica et Cosmochimica Acta, 52(2): 475-483.

Bargar, K.E., 1978. Geology and Thermal History of Mammoth Hot Springs, Yellowstone National Park, Wyoming. U. S. Geological Survey Bulletin 1444.

Bergfeld, D., Lowenstern, J.B., Hunt, A.G., Hurwitz, S., McCleskey, B.R. and Peek, S.E., 2019. Chemical and isotopic data on gases and waters for thermal and non-thermal features across Yellowstone National Park (ver. 2.0, March 2019). U.S. Geological Survey data release, https://doi.org/10.5066/F7H13105.

Bowell, R.J., Alpers, C.N., Jamieson, H.E., Nordstrom, D.K. and Majzlan, J., 2014. The environmental geochemistry of arsenic—an overview. Reviews in Mineralogy and Geochemistry, 79.

Boyd, E., Fecteau, K., Havig, J., Shock, E. and Peters, J., 2012. Modeling the habitat range of phototrophs in Yellowstone National Park: Toward the development of a comprehensive fitness landscape. Frontiers in Microbiology, 3(221).
Brock, T.D., 1971. Bimodal distribution of pH values of thermal springs of the world. GSA Bulletin, 82(5): 1393-1394.
Brock, T.D., 1994. Life at High Temperatures. Yellowstone Association, Mammoth, WY.
Campbell, K.M. and Nordstrom, D.K., 2014. Arsenic speciation and sorption in natural environments. Reviews in Mineralogy and Geochemistry, 79(1): 185-216.
Chaffee, M., Shanks, W., Rye, R., Schwartz, C., Adams, M., Carlson, R., Crock, J., Gemery-Hill, P., Gunther, K., Kester, C., King, H. and Podruzny, S., 2007. Applications of trace-element and stable-isotope geochemistry to wildlife issues, Yellowstone National Park and vicinity, Chapter J in Integrated geoscience studies in the greater Yellowstone area—volcanic, tectonic, and hydrothermal processes in the Yellowstone geoecosystem. U.S. Geological Survey Professional Paper 1717.
Cherry, J.A., Shaikh, D.E., Tallman, D.E. and Nicholson, R.V., 1979. Arsenic species as an indicator of redox conditions in groundwater. Journal of Hydrology, 43: 373-392.
Christiansen, R.L., 2001. The Quaternary and Pliocene Yellowstone Plateau volcanic field of Wyoming, Idaho, and Montana. U.S. Geological Survey Professional Paper 729-G.
Churchill, D.M., Manga, M., Hurwitz, S., Peek, S., Damby, D.E., Conrey, R., Wood, J.R., McCleskey, R.B., Keller, W.E., Hosseini, B. and Hungerford, J.D.G., 2021a. The structure and volume of large geysers in Yellowstone National Park, USA and the mineralogy and chemistry of their silica sinter deposits. Journal of Volcanology and Geothermal Research, 419: 107391.
Churchill, D.M., Peek, S.E., Hurwitz, S., Manga, M., Damby, D.E., Conrey, R., Paces, J.B. and Licciardi, J.M., 2021b. Mineralogy, chemistry and isotope composition of silica sinter deposits from the Upper Geyser Basin, Yellowstone National Park (ver. 2.0, April 2021). U.S. Geological Survey data release, https://doi.org/10.5066/P90SU3TV.
Colman, D.R., Amenabar, M.J., Fernandes-Martins, M.C. and Boyd, E.S., 2022. Subsurface Archaea associated with rapid geobiological change in a model Yellowstone hot spring. Communications Earth & Environment, 3(1): 205.
Colman, D.R., Feyhl-Buska, J., Robinson, K.J., Fecteau, K.M., Xu, H., Shock, E.L. and Boyd, E.S., 2016. Ecological differentiation in planktonic and sediment-associated chemotrophic microbial populations in Yellowstone hot springs. FEMS Microbiology Ecology, 92(9).
Colman, D.R., Lindsay, M.R., Amenabar, M.J. and Boyd, E.S., 2019. The intersection of geology, geochemistry, and microbiology in continental hydrothermal systems. Astrobiology, 19(12): 1505-1522.
Colman, D.R., Lindsay, M.R., Amenabar, M.J., Fernandes-Martins, M.C., Roden, E.R. and Boyd, E.S., 2020. Phylogenomic analysis of novel Diaforarchaea is consistent with sulfite but not sulfate reduction in volcanic environments on early Earth. The ISME Journal, 14(5): 1316-1331.
Cox, A., Shock, E.L. and Havig, J.R., 2011. The transition to microbial photosynthesis in hot spring ecosystems. Chemical Geology, 280(3): 344-351.
Cozen, A.E., Weirauch, M.T., Pollard, K.S., Bernick, D.L., Stuart, J.M. and Lowe, T.M., 2009. Transcriptional map of respiratory versatility in the Hyperthermophilic Crenarchaeon *Pyrobaculum aerophilum*. Journal of Bacteriology, 191(3): 782-794.

Cullen, J.T., 2020. Chemistry-Isotopes-Yellowstone. Texas Data Repository, University of Texas at Austin Dataverse Collection, https://doi.org/10.18738/T8/ULLRE3, University of Texas at Austin Dataverse Collection.

Cullen, J.T., Hurwitz, S., Barnes, J.D., Lassiter, J.C., Penniston-Dorland, S., Kasemann, S.A. and Thordsen, J.J., 2019. Temperature-dependent variations in mineralogy, major element chemistry and the stable isotopes of boron, lithium and chlorine resulting from hydration of rhyolite: Constraints from hydrothermal experiments at 150 to 350 °C and 25 MPa. Geochimica et Cosmochimica Acta, 261: 269-287.

Cullen, J.T., Hurwitz, S., Barnes, J.D., Lassiter, J.C., Penniston-Dorland, S., Meixner, A., Wilckens, F., Kasemann, S.A. and McCleskey, R.B., 2021. The systematics of chlorine, lithium, and boron and $\delta^{37}Cl$, $\delta^{7}Li$, and $\delta^{11}B$ in the hydrothermal system of the Yellowstone Plateau Volcanic Field. Geochemistry, Geophysics, Geosystems, 22(4): e2020GC009589.

D'Imperio, S., Lehr, C.R., Breary, M. and McDermott, T.R., 2007. Autoecology of an arsenite chemolithotroph: Sulfide constraints on function and distribution in a geothermal spring. Applied and Environmental Microbiology, 73(21): 7067–7074.

Danczak, R.E., Johnston, M.D., Kenah, C., Slattery, M. and Wilkins, M.J., 2019. Capability for arsenic mobilization in groundwater is distributed across broad phylogenetic lineages. PloS one, 14(9): e0221694-e0221694.

Donahoe-Christiansen, J., D'Imperio, S., Jackson, C.R., Inskeep, W.P. and McDermott, T.R., 2004. Arsenite-oxidizing *Hydrogenobaculum* strain isolated from an acid-sulfate-chloride geothermal spring in Yellowstone National Park. Applied and Environmental Microbiology, 70(3): 1865-1868.

Ellis, A.J. and Mahon, W.A.J., 1964. Natural hydrothermal systems and experimental hot water/rock interactions. Geochimica et Cosmochimica Acta, 28: 1323–1357.

Ellis, A.J. and Mahon, W.A.J., 1977. Chemistry and geothermal systems. Academic Press, New York, NY, 392 pp.

Ewers, G.R., 1977. Experimental hot water-rock interactions and their significance to natural hydrothermal systems in New Zealand. Geochimica et Cosmochimica Acta, 41(1): 143-150.

Farrell, J., Smith, R.B., Husen, S. and Diehl, T., 2014. Tomography from 26 years of seismicity revealing that the spatial extent of the Yellowstone crustal magma reservoir extends well beyond the Yellowstone caldera. Geophysical Research Letters, 41(9): 3068-3073.

Fecteau, K.M., Boyd, E.S., Lindsay, M.R., Amenabar, M.J., Robinson, K.J., Debes II, R.V. and Shock, E.L., 2022. Cyanobacteria and Algae Meet at the Limits of Their Habitat Ranges in Moderately Acidic Hot Springs. Journal of Geophysical Research: Biogeosciences, 127(1): e2021JG006446.

Feth, J.H., 1981. Chloride in natural continental water--A review. U.S. Geological Survey Water Supply Paper 2176, Washington, D.C.

Finkelshtein, A.L. and Chubarov, V.M., 2010. X-ray fluorescence determination of the FeO/Fe2O3tot ratio in igneous rocks. X-Ray Spectrometry, 39(1): 17-21.

Floquet, C.F., Sieben, V.J., MacKay, B.A. and Mostowfi, F., 2016. Determination of boron concentration in oilfield water with a microfluidic ion exchange resin instrument. Talanta, 154: 304-11.

Fouke, B.W., Farmer, J.D., Des Marais, D.J., Pratt, L., Sturchio, N.C., Burns, P.C. and Discipulo, M.K., 2000. Depositional facies and aqueous-solid geochemistry of travertine-

depositing hot springs (Angel Terrace, Mammoth Hot Springs, Yellowstone National Park, U.S.A.). Journal of Sedimentary Research, 70(3): 565-585.
Fournier, R.O., 1977. Chemical geothermometers and mixing models for geothermal systems. Geothermics, 5: 41-50.
Fournier, R.O., 1989. Geochemistry and dynamics of the Yellowstone National Park hydrothermal system. Annual Reviews of Earth and Planetary Science, 17: 13-53.
Fournier, R.O., 2005. Geochemistry and dynamics of the Yellowstone National Park hydrothermal system. In: W.P. Inskeep and T.R. McDermott (Editors), Geothermal Biology and Geochemistry in Yellowstone National Park. MSU Thermal Biology Institute, Montana State University, Bozeman, MT, pp. 3-30.
Friedman, I. and Norton, D.R., 1990. Anomalous chloride flux discharges from Yellowstone National Park. Journal of Volcanology and Geothermal Research, 42(3): 225-234.
Garelick, H., Jones, H., Dybowska, A. and Valsami-Jones, E., 2008. Arsenic pollution sources. Rev Environ Contam Toxicol, 197: 17-60.
Gemery-Hill, P.A., Shanks III, W., Balistrieri, L. and Lee, G., 2007. Geochemical data for selected rivers, lake waters, hydrothermal vents, and subaerial geysers in Yellowstone National Park, Wyoming and Vicinity, 1996–2004. In: L.A. Morgan (Editor), Integrated Geoscience Studies in the Greater Yellowstone Area—Volcanic, Tectonic, and Hydrothermal Processes in the Yellowstone Geoecosystem, pp. 367-426.
Gihring, T.M. and Banfield, J.F., 2001. Arsenite oxidation and arsenate respiration by a new Thermus isolate. FEMS Microbiology Letters, 204(2): 335-340.
Gihring, T.M., Druschel, G.K., McCleskey, R.B., Hamers, R.J. and Banfield, J.F., 2001. Rapid arsenite oxidation by *Thermus aquaticus* and *Thermus thermophilus*: field and laboratory investigations. Environmental Science & Technology, 35(19): 3857-3862.
Goeff, F. and Gardner, J.N., 1994. Evolution of a mineralized geothermal system, Valles Caldera, New Mexico. Economic Geology, 89(8): 1803-1832.
Goldstein, J.N., Hubert, W.A., Woodward, D.F., Farag, A.M. and Meyer, J.S., 2001. Naturalized salmonid populations occur in the presence of elevated trace element concentrations and temperatures in the firehole river, yellowstone National Park, Wyoming, USA. Environmental Toxicology and Chemistry, 20(10): 2342-2352.
Gooch, F.A. and Whitfield, J.E., 1888. Analyses of waters of the Yellowstone National Park with an account of the methods of analysis employed. U.S. Geological Survey Bulletin 47.
Guo, Q., Planer-Friedrich, B., Liu, M., Li, J., Zhou, C. and Wang, Y., 2017. Arsenic and thioarsenic species in the hot springs of the Rehai magmatic geothermal system, Tengchong volcanic region, China. Chemical Geology, 453: 12-20.
Hague, A., 1887. Notes on the deposition of scorodite from arsenical waters in the Yellowstone National Park. American Journal of Science, 34: 171-175.
Hague, A., 1911. The Origin of the Thermal Waters in the Yellowstone National Park. Science, 33(850): 553-568.
Hamamura, N., Macur, R.E., Korf, S., Ackerman, G., Taylor, W.P., Kozubal, M., Reysenbach, A.L. and Inskeep, W.P., 2009. Linking microbial oxidation of arsenic with detection and phylogenetic analysis of arsenite oxidase genes in diverse geothermal environments. Environmental Microbiology, 11(2): 421-31.
Hamilton, T.L., Vogl, K., Bryant, D.A., Boyd, E.S. and Peters, J.W., 2012. Environmental constraints defining the distribution, composition, and evolution of chlorophototrophs in thermal features of Yellowstone National Park. Geobiology, 10(3): 236-49.

Harrison, L.N., Hurwitz, S., Paces, J.B., McCleskey, R.B., Roth, D.A., Conrey, R. and Stelten, M.E., 2022. Elemental and strontium isotopic composition of select Central Plateau and Upper Basin Member Rhyolites, Yellowstone Plateau Volcanic Field. U.S. Geological Survey data release, https://doi.org/10.5066/P952ZE74.

Härtig, C., Lohmayer, R., Kolb, S., Horn, M.A., Inskeep, W.P. and Planer-Friedrich, B., 2014. Chemolithotrophic growth of the aerobic hyperthermophilic bacterium Thermocrinis ruber OC 14/7/2 on monothioarsenate and arsenite. FEMS Microbiology Ecology, 90(3): 747-60.

Hingston, F.J., Posner, A.M. and Quirk, J.P., 1971. Competitive adsorption of negatively charged ligands on oxide surfaces. Discussions of the Faraday Society 52: 334 - 342.

Holloway, J.M., Nordstrom, D.K., Böhlke, J.K., McCleskey, R.B. and Ball, J.W., 2011. Ammonium in thermal waters of Yellowstone National Park: Processes affecting speciation and isotope fractionation. Geochimica et Cosmochimica Acta, 75(16): 4611-4636.

Huber, R., Sacher, M., Vollmann, A., Huber, H. and Rose, D., 2000. Respiration of arsenate and selenate by hyperthermophilic archaea. Systematic and Applied Microbiology, 23(3): 305-314.

Hurwitz, S., Eagan, S., Heasler, H., Mahony, D., Huebner, M.A. and Lowenstern, J.B., 2007. River chemistry and solute flux in Yellowstone National Park. U.S. Geological Survey Data Series 278, Version 3.0.

Hurwitz, S., Harris, R.N., Werner, C.A. and Murphy, F., 2012a. Heat flow in vapor dominated areas of the Yellowstone Plateau Volcanic Field: Implications for the thermal budget of the Yellowstone Caldera. Journal of Geophysical Research: Solid Earth, 117(B10).

Hurwitz, S., Hunt, A.G. and Evans, W.C., 2012b. Temporal variations of geyser water chemistry in the Upper Geyser Basin, Yellowstone National Park, USA. Geochemistry, Geophysics, Geosystems, 13(12).

Hurwitz, S. and Lowenstern, J.B., 2014. Dynamics of the Yellowstone hydrothermal system. Reviews of Geophysics, 52(3): 375-411.

Hurwitz, S., McCleskey, R.B., Bergfeld, D., Peek, S.E., Susong, D.D., Roth, D.A., Hungerford, J.D.G., White, E.B., Harrison, L.N., Hosseini, B., Vaughan, R.G., Hunt, A.G. and Paces, J.B., 2020. Hydrothermal activity in the southwest Yellowstone Plateau Volcanic Field. Geochemistry, Geophysics, Geosystems, 21: e2019GC008848.

Ingebritsen, S.E. and Evans, W.C., 2019. Potential for increased hydrothermal arsenic flux during volcanic unrest: Implications for California water supply. Applied Geochemistry, 108: 104384.

Inskeep, W., Jay, Z., Tringe, S., Herrgard, M. and Rusch, D., 2013. The YNP Metagenome Project: Environmental parameters responsible for microbial distribution in the Yellowstone geothermal ecosystem. Frontiers in Microbiology, 4(67).

Inskeep, W.P., Macur, R.E., Hamamura, N., Warelow, T.P., Ward, S.A. and Santini, J.M., 2007. Detection, diversity and expression of aerobic bacterial arsenite oxidase genes. Environmental Microbiology, 9(4): 934-43.

Inskeep, W.P., Macur, R.E., Harrison, G., Bostick, B.C. and Fendorf, S., 2004. Biomineralization of As(V)-hydrous ferric oxyhydroxide in microbial mats of an acid-sulfate-chloride geothermal spring, Yellowstone National Park1 1Associate editor: L. B. Benning. Geochimica et Cosmochimica Acta, 68(15): 3141-3155.

Jay, Z.J., Beam, J.P., Dohnalkova, A., Lohmayer, R., Bodle, B., Planer-Friedrich, B., Romine, M., Inskeep, W.P. and Voordouw, G., 2015. Pyrobaculum yellowstonensis strain WP30 respires on elemental sulfur and/or arsenate in circumneutral sulfidic geothermal sediments of Yellowstone National Park. Applied and Environmental Microbiology, 81(17): 5907-5916.

Jay, Z.J., Beam, J.P., Kozubal, M.A., Jennings, R.d., Rusch, D.B. and Inskeep, W.P., 2016. The distribution, diversity and function of predominant Thermoproteales in high-temperature environments of Yellowstone National Park. Environmental Microbiology, 18(12): 4755-4769.

Jiang, Z., Li, P., Jiang, D., Wu, G., Dong, H., Wang, Y., Li, B., Wang, Y. and Guo, Q., 2014. Diversity and abundance of the arsenite oxidase gene aioA in geothermal areas of Tengchong, Yunnan, China. Extremophiles, 18(1): 161-70.

Johnson, P., 2016. Yellowstone grapples with high arsenic levels In 'Old Faithful' water supply, Water Online.

Kharaka, Y.K., Sorey, M.L. and Thordsen, J.J., 2000. Large-scale hydrothermal fluid discharges in the Norris–Mammoth corridor, Yellowstone National Park, USA. Journal of Geochemical Exploration, 69-70: 201-205.

King, J.M., Hurwitz, S., Lowenstern, J.B., Nordstrom, D.K. and McCleskey, R.B., 2016. Multireaction equilibrium geothermometry: A sensitivity analysis using data from the Lower Geyser Basin, Yellowstone National Park, USA. Journal of Volcanology and Geothermal Research, 328: 105-114.

Kocar, B.D., Garrott, R.A. and Inskeep, W.P., 2004. Elk exposure to arsenic in geothermal watersheds of Yellowstone National Park, USA. Environ Toxicol Chem, 23(4): 982-9.

Kumari, N. and Jagadevan, S., 2016. Genetic identification of arsenate reductase and arsenite oxidase in redox transformations carried out by arsenic metabolising prokaryotes - A comprehensive review. Chemosphere, 163: 400-412.

Landrum, J.T., Bennett, P.C., Engel, A.S., Alsina, M.A., Pastén, P.A. and Milliken, K., 2009. Partitioning geochemistry of arsenic and antimony, El Tatio Geyser Field, Chile. Applied Geochemistry, 24(4): 664-676.

Langner, H.W., Jackson, C.R., McDermott, T.R. and Inskeep, W.P., 2001. Rapid Oxidation of Arsenite in a Hot Spring Ecosystem, Yellowstone National Park. Environmental Science & Technology, 35: 3302-3309.

López, D.L., Bundschuh, J., Birkle, P., Armienta, M.A., Cumbal, L., Sracek, O., Cornejo, L. and Ormachea, M., 2012. Arsenic in volcanic geothermal fluids of Latin America. Science of The Total Environment, 429: 57-75.

Love, J.D. and Good, J.M., 1970. Hydrocarbons in thermal areas, northwestern Wyoming. U.S. Geological Survey Professional Paper 644-B.

Love, J.D. and Keefer, W.R., 1975. Geology of sedimentary rocks in southern Yellowstone National Park, Wyoming. U.S. Geological Survey Professional Paper 729-D.

Lowenstern, J.B., Bergfeld, D., Evans, W.C. and Hunt, A.G., 2015. Origins of geothermal gases at Yellowstone. Journal of Volcanology and Geothermal Research, 302: 87-101.

Lowenstern, J.B., Bergfeld, D., Evans, W.C. and Hurwitz, S., 2012. Generation and evolution of hydrothermal fluids at Yellowstone: Insights from the Heart Lake Geyser Basin. Geochemistry, Geophysics, Geosystems, 13(Q01017): 1-20.

Macur, R.E., Langner, H.W., Kocar, B.D. and Inskeep, W.P., 2004. Linking geochemical processes with microbial community analysis: successional dynamics in an arsenic-rich, acid-sulphate-chloride geothermal spring. Geobiology, 2(3): 163-177.

Marini, L., Vetuschi Zuccolini, M. and Saldi, G., 2003. The bimodal pH distribution of volcanic lake waters. Journal of Volcanology and Geothermal Research, 121: 83-98.

McCleskey, R.B., Ball, J.W. and Nordstrom, D.K., 2003. Metal interferences and their removal prior to the determination of As(T) and As(III) in acid mine waters by hydride generation atomic absorption spectrometry. U.S. Geological Survey Water-Resources Investigations Report 03-4117.

McCleskey, R.B., Ball, J.W., Nordstrom, D.K., Holloway, J.M. and Taylor, H.E., 2005. Water-chemistry data for selected springs, geysers, and streams in Yellowstone National Park, Wyoming, 2001-2002. U.S. Geological Survey Open-File Report 2004-1316.

McCleskey, R.B., Chiu, R.B., Nordstrom, D.K., Campbell, K.M., Roth, D.A., Ball, J.W. and Plowman, T.I., 2014. Water-chemistry data for selected springs, geysers, and streams in Yellowstone National Park, Wyoming, Beginning 2009. [doi:10.5066/F7M043FS].

McCleskey, R.B., Clor, L.E., Lowenstern, J.B., Evans, W.C., Nordstrom, D.K., Heasler, H. and Huebner, M.A., 2012. Solute and geothermal flux monitoring using electrical conductivity in the Madison, Firehole, and Gibbon Rivers, Yellowstone National Park. Applied Geochemistry, 27(12): 2370-2381.

McCleskey, R.B., Hurwitz, S., White, E.B., Roth, D.A., Susong, D.D., Hungerford, J.D.G. and Olson, L.A., 2020. Sources, fate, and flux of riverine solutes in the Southwest Yellowstone Plateau Volcanic Field, USA. Journal of Volcanology and Geothermal Research, 403: 107021.

McCleskey, R.B., Lowenstern, J.B., Schaper, J., Nordstrom, D.K., Heasler, H.P. and Mahony, D., 2016. Geothermal solute flux monitoring and the source and fate of solutes in the Snake River, Yellowstone National Park, WY. Applied Geochemistry, 73: 142-156.

McCleskey, R.B., Nordstrom, D.K. and Maest, A.S., 2004. Preservation of water samples for arsenic(III/V) determinations: an evaluation of the literature and new analytical results. Applied Geochemistry, 19(7): 995-1009.

McCleskey, R.B., Nordstrom, D.K., Susong, D.D., Ball, J.W. and Taylor, H.E., 2010. Source and fate of inorganic solutes in the Gibbon River, Yellowstone National Park, Wyoming, USA. II. Trace element chemistry. Journal of Volcanology and Geothermal Research, 196(3-4): 139-155.

McCleskey, R.B., Roth, D.A., Hurwitz, S., Bergfeld, D., Peek, S.E., Susong, D.D., White, E.B., Hungerford, J., Hunt, A.G., Paces, J.B. and Olson, L., 2019a. Water chemistry data for selected hot springs and rivers in Southwest Yellowstone National Park, Wyoming. U.S. Geological Survey Data Release, https://doi.org/10.5066/P9MJ0HYM.

McCleskey, R.B., Roth, D.A., Mahony, D., Nordstrom, D.K. and Kinsey, S., 2019b. Sources, fate, and flux of geothermal solutes in the Yellowstone and Gardner Rivers, Yellowstone National Park, WY. Applied Geochemistry, 111: 104458.

McCleskey, R.B., Roth, D.A., Nordstrom, D.K., Hurwitz, S., Holloway, J.M., Bliznik, P.A., Ball, J.W. and Repert, D.A., 2022. Water-chemistry and isotope data for selected springs, geysers, streams, and rivers in Yellowstone National Park, Wyoming. U.S. Geological Survey data release, https://doi.org/10.5066/P92XKJU7.

McCleskey, R.B., White, E.B., Roth, D.A. and Stevens, E.B., 2019c. Specific conductance data for selected rivers and creeks in Yellowstone National Park, beginning in 2010 (version 2.0, May 2020): U.S. Geological Survey data release, https://doi.org/10.5066/F7BP011G.
McEwan, A.G., Ridge, J.P., McDevitt, C.A. and Hugenholtz, P., 2002. The DMSO Reductase Family of Microbial Molybdenum Enzymes; Molecular Properties and Role in the Dissimilatory Reduction of Toxic Elements. Geomicrobiology Journal, 19(1): 3-21.
Mikael Sehlin, H. and Börje Lindström, E., 1992. Oxidation and reduction of arsenic by Sulfolobus acidocaldarius strain BC. FEMS Microbiology Letters, 93(1): 87-92.
Miller, K.A., Clark, M.L. and Wright, P.R., 2004. Water-quality assessment of the Yellowstone River Basin, Montana and Wyoming – water quality of fixed sites, 1999-2001. U.S. Geological Survey Scientific Investigations Report 2004-5113.
Montana Department of Environmental Quality, 1995. Montana numeric water quality standards. Water Quality Division Circular WQB-7, Helena, Montana.
Montana Department of Environmental Quality, 2018. Demonstration of nonanthropogenic arsenic: Yellowstone River, Montana. WQSMTECH-01.
Morales-Simfors, N., Bundschuh, J., Herath, I., Inguaggiato, C., Caselli, A.T., Tapia, J., Choquehuayta, F.E.A., Armienta, M.A., Ormachea, M., Joseph, E. and López, D.L., 2020. Arsenic in Latin America: A critical overview on the geochemistry of arsenic originating from geothermal features and volcanic emissions for solving its environmental consequences. Science of The Total Environment, 716: 135564.
Morales, I., Villanueva-Estrada, R.E., Rodríguez, R. and Armienta, M.A., 2015. Geological, hydrogeological, and geothermal factors associated to the origin of arsenic, fluoride, and groundwater temperature in a volcanic environment “El Bajío Guanajuatense”, Mexico. Environmental Earth Sciences, 74(6): 5403-5415.
Muramatsu, F., Tonomura, M., Yamada, M., Kasahara, Y., Yamamura, S., Iino, T. and Amachi, S., 2020. Possible involvement of a tetrathionate reductase homolog in dissimilatory arsenate reduction by anaeromyxobacter sp. strain PSR-1. Appl Environ Microbiol, 86(23).
National Park Service, 2020. Old Faithful Water Quality Report - Annual Drinking Water Quality Report for 2020. Old Faithful — Yellowstone National Park — Public Water System 5680085.
Nguyen, L.T., Schmidt, H.A., von Haeseler, A. and Minh, B.Q., 2015. IQ-TREE: a fast and effective stochastic algorithm for estimating maximum-likelihood phylogenies. Molecular Biology and Evolution, 32(1): 268-74.
Nimick, D.A., Moore, J.N., Dalby, C.E. and Savka, M.W., 1998. The fate of geothermal arsenic in the Madison and Missouri Rivers, Montana and Wyoming. Water Resources Research, 34(11): 3051-3067.
Nordstrom, D.K., 2002. Worldwide occurrences of arsenic in ground water. Science, 296(5576): 2143-2145.
Nordstrom, D.K., Ball, J.W. and McCleskey, R.B., 2003. Orpiment solubility equilibrium and arsenic speciation for a hot spring at Yellowstone National Park using revised thermodynamic data, Geological Society of America Annual Meeting, Seattle, WA.
Nordstrom, D.K., Ball, J.W. and McCleskey, R.B., 2005. Ground water to surface water: chemistry of thermal outflows in Yellowstone National Park. In: W.P. Inskeep and T.R. McDermott (Editors), Geothermal biology and geochemistry in Yellowstone National

Park. Thermal Biology Institute and Department of Land Resources and Environmental Sciences, Montana State University, Bozeman, Montana, pp. 73-94.
Nordstrom, D.K., McCleskey, R.B. and Ball, J.W., 2001. Processes governing arsenic geochemistry in the thermal waters of Yellowstone National Park, USGS Workshop on Arsenic in the Environment, Denver, CO.
Nordstrom, D.K., McCleskey, R.B. and Ball, J.W., 2009. Sulfur geochemistry of hydrothermal waters in Yellowstone National Park, Wyoming, USA. IV. Acid-sulfate waters. Applied Geochemistry, 24(2): 191-207.
Onishi, H. and Sandell, E.B., 1955. Geochemistry of arsenic. Geochimica et Cosmochimica Acta, 7(1): 1-33.
Oremland, R.S. and Stolz, J., 2000. Dissimilatory reduction of selenate and arsenate in nature, Environmental Microbe-Metal Interactions, pp. 199-224.
Parkhurst, D.L. and Appelo, C.A.J., 1999. User's guide to PHREEQC (Version 2) - A computer program for speciation, batch-reaction, one-dimensional transport, and inverse geochemical calculations. U.S. Geological Survey Water-Resources Investigations Report 99-4259.
Planer-Friedrich, B., Forberg, J., Lohmayer, R., Kerl, C.F., Boeing, F., Kaasalainen, H. and Stefánsson, A., 2020. Relative abundance of thiolated species of As, Mo, W, and Sb in hot springs of Yellowstone National Park and Iceland. Environmental Science & Technology, 54(7): 4295-4304.
Planer-Friedrich, B., Lehr, C., Matschullat, J., Merkel, B.J., Nordstrom, D.K. and Sandstrom, M.W., 2006. Speciation of volatile arsenic at geothermal features in Yellowstone National Park. Geochimica et Cosmochimica Acta, 70(10): 2480-2491.
Planer-Friedrich, B., London, J., McCleskey, R.B., Nordstrom, D.K. and Wallschlaeger, D., 2007. Thioarsenates in geothermal waters of Yellowstone National Park: determination, preservation, and geochemical importance. Environmental Science & Technology, 41(15): 5245-5251.
Planer-Friedrich, B. and Wallschläger, D., 2009. A Critical Investigation of Hydride Generation-Based Arsenic Speciation in Sulfidic Waters. Environmental Science & Technology, 43(13): 5007-5013.
Qin, J., Lehr, C.R., Yuan, C., Le, X.C., McDermott, T.R. and Rosen, B.P., 2009. Biotransformation of arsenic by a Yellowstone thermoacidophilic eukaryotic alga. Proceedings of the National Academy of Sciences, 106(13): 5213-5217.
Reid, K.D., Goff, F. and Counce, D.A., 2003. Arsenic concentration and mass flow rate in natural waters of the Valles caldera and Jemez Mountains region, New Mexico. New Mexico Geology, 25(3): 75-81.
Robinson, B., Kim, N., Marchetti, M., Moni, C., Schroeter, L., van den Dijssel, C., Milne, G. and Clothier, B., 2006. Arsenic hyperaccumulation by aquatic macrophytes in the Taupo Volcanic Zone, New Zealand. Environmental and Experimental Botany, 58(1): 206-215.
Roth, D.A., Johnson, M.O., McCleskey, R.B., Riskin, M.L. and Bliznik, P.A., 2022. Evaluation of preservation techniques for trace metals and major cations for surface waters collected from the U.S. Geological Survey's National Water Quality Network Sites. U.S. Geological Survey data release, https://doi.org/10.5066/P9SMPZ3M.
Sanchez-Yanez, C., Reich, M., Leisen, M., Morata, D. and Barra, F., 2017. Geochemistry of metals and metalloids in siliceous sinter deposits: Implications for elemental partitioning into silica phases. Applied Geochemistry, 80: 112-133.

Sayers, E.W., Bolton, E.E., Brister, J.R., Canese, K., Chan, J., Comeau, D.C., Connor, R., Funk, K., Kelly, C., Kim, S., Madej, T., Marchler-Bauer, A., Lanczycki, C., Lathrop, S., Lu, Z., Thibaud-Nissen, F., Murphy, T., Phan, L., Skripchenko, Y., Tse, T., Wang, J., Williams, R., Trawick, B.W., Pruitt, K.D. and Sherry, S.T., 2022. Database resources of the national center for biotechnology information. Nucleic Acids Res, 50(D1): D20-d26.

Segerer, A.H., Trincone, A., Gahrtz, M. and Stetter, K.O., 1991. Stygiolobus azoricus gen. nov., sp. nov. Represents a novel genus of anaerobic, extremely thermoacidophilic archaebacteria of the order sulfolobales. International Journal of Systematic and Evolutionary Microbiology, 41(4): 495-501.

Sehlin, H.M. and Lindström, E.B., 1992. Oxidation and reduction of arsenic by Sulfolobus acidocaldarius strain BC. FEMS Microbiology Letters, 93(1): 87-92.

Sherman, L.S., Blum, J.D., Nordstrom, D.K., McCleskey, R.B., Barkay, T. and Vetriani, C., 2009. Mercury isotopic composition of hydrothermal systems in the Yellowstone Plateau volcanic field and Guaymas Basin sea-floor rift. Earth and Planetary Science Letters, 279(1): 86-96.

Shock, E.L., Holland, M., Meyer-Dombard, D.A., Amend, J.P., Osburn, G.R. and Fischer, T.P., 2010. Quantifying inorganic sources of geochemical energy in hydrothermal ecosystems, Yellowstone National Park, USA. Geochimica et Cosmochimica Acta, 74(14): 4005-4043.

Sievers, F., Wilm, A., Dineen, D., Gibson, T.J., Karplus, K., Li, W., Lopez, R., McWilliam, H., Remmert, M., Söding, J., Thompson, J.D. and Higgins, D.G., 2011. Fast, scalable generation of high-quality protein multiple sequence alignments using Clustal Omega. Molecular systems biology, 7: 539-539.

Smedley, P.L. and Kinniburgh, D.G., 2002. A review of the source, behaviour and distribution of arsenic in natural waters. Applied Geochemistry, 17(5): 517-568.

Smieja, J.A. and Wilkin, R.T., 2003. Preservation of sulfidic waters containing dissolved As(III). Journal of Environmental Monitoring, 5(6): 913-916.

Smith, R.B., Jordan, M., Steinberger, B., Puskas, C.M., Farrell, J., Waite, G.P., Husen, S., Chang, W.-L. and O'Connell, R., 2009. Geodynamics of the Yellowstone hotspot and mantle plume: Seismic and GPS imaging, kinematics, and mantle flow. Journal of Volcanology and Geothermal Research, 188(1): 26-56.

Stauffer, R.E., 1980. Molybdenum blue applied to arsenic and phosphorous determinations in fluoride- and silica-rich geothermal waters. Environmental Science & Technology, 14: 1475-1481.

Stauffer, R.E., Jenne, E.A. and Ball, J.W., 1980. Chemical studies of selected trace elements in hot-spring drainages of Yellowstone National Park. U.S. Geological Survey Professional Paper 1044-F.

Stauffer, R.E. and Thompson, J.M., 1984. Arsenic and antimony in geothermal waters of Yellowstone National Park, Wyoming, USA. Geochimica et Cosmochimica Acta, 48: 2247-2561.

Stolz, J.F., Basu, P., Santini, J.M. and Oremland, R.S., 2006. Arsenic and selenium in microbial metabolism. Annual Review of Microbiology, 60: 107-30.

Stolz, J.F. and Oremland, R.S., 1999. Bacterial respiration of arsenic and selenium. FEMS Microbiology Reviews, 23(5): 615-627.

Summers Engel, A., Johnson, L.R. and Porter, M.L., 2013. Arsenite oxidase gene diversity among Chloroflexi and Proteobacteria from El Tatio Geyser Field, Chile. FEMS Microbiology Ecology, 83(3): 745-756.

Takacs-vesbach, C., Inskeep, W., Jay, Z., Herrgard, M., Rusch, D., Tringe, S., Kozubal, M., Hamamura, N., Macur, R., Fouke, B., Reysenbach, A.-L., McDermott, T., Jennings, R., Hengartner, N. and Xie, G., 2013. Metagenome sequence analysis of filamentous microbial communities obtained from geochemically distinct geothermal channels reveals specialization of three aquificales lineages. Frontiers in Microbiology, 4(84).

Tec-Caamal, E.N., Rodríguez-Vázquez, R. and Aguilar-López, R., 2019. Kinetic analysis of arsenic and iron oxidation by Acidianus brierleyi for biogenic scorodite formation. Chemical Papers, 73(4): 811-820.

Thompson, J.M., 1979. Arsenic and fluoride in the upper Madison River system: Firehole and Gibbon Rivers and their tributaries, Yellowstone National Park, Wyoming, and Southeast Montana. Environmental Geology, 3(1): 13-21.

Thompson, J.M. and DeMonge, J.M., 1996. Chemical analyses of hot springs, pools, and geysers from Yellowstone National Park, Wyoming, and vicinity, 1980-1993. U.S. Geological Survey Open-File Report 96-68.

Thompson, J.M. and Hutchinson, R.A., 1981. Chemical analyses of waters from the Boundary Creek thermal area, Yellowstone National Park, Wyoming. US Geological Survey, Open-File Report 81-1310.

Thompson, J.M., Keith, T.E.C. and Consul, J.J., 1985. Water chemistry and mineralogy of Morgan and Growler Hot Springs, Lassen KGRA, California. Transactions of the Geothermal Research Council, 9: 357–362.

U.S. Geological Survey, 2021. USGS water data for the Nation: U.S. Geological Survey National Water Information System database. https://doi.org/10.5066/F7P55KJN.

Uhlig, S., Möckel, R. and Pleßow, A., 2016. Quantitative analysis of sulphides and sulphates by WD-XRF: Capability and constraints. X-Ray Spectrometry, 45(3): 133-137.

Vaughan, R.G., Heasler, H., Jaworowski, C., Lowenstern, J.B. and Keszthelyi, L.P., 2013. Provisional maps of thermal areas in Yellowstone National Park, based on satellite thermal infrared imaging and field observations. U.S. Geological Survey Scientific Investigations Report 2014–5137.

Webster, J.G. and Nordstrom, D.K., 2003. Geothermal arsenic. In: A.H. Welch and K.G. Stollenwerk (Editors), Arsenic in ground water: geochemistry and occurrence. Springer Science & Business Media, Boston, Massachusetts.

Weed, W.H. and Pirsson, L.V., 1891. Occurrence of sulphur, orpiment, and realgar in the Yellowstone National Park. American Journal of Science, 42: 401-405.

Werner, C., Hurwitz, S., Evans, W.C., Lowenstern, J.B., Bergfeld, D., Heasler, H., Jaworowski, C. and Hunt, A., 2008. Volatile emissions and gas geochemistry of Hot Spring Basin, Yellowstone National Park, USA. Journal of Volcanology and Geothermal Research, 178(4): 751-762.

White, D.E., Fournier, R.O., Muffler, L.J.P. and Truesdell, A.H., 1975. Physical results of research drilling in thermal areas of Yellowstone National Park, Wyoming. U.S. Geological Survey Professional Paper 892.

White, D.E., Hutchinson, R.A. and Keith, T.E.C., 1988. The geology and remarkable thermal activity of Norris Geyser Basin, Yellowstone National Park, Wyoming. U.S. Geological Survey Professional Paper 1456.

White, D.E., Muffler, L.J.P. and Truesdell, A.H., 1971. Vapor-dominated hydrothermal systems compared with hot-water systems. Economic Geology, 66(1): 75-97.
Wilkie, J.A. and Hering, J.G., 1998. Rapid oxidation of geothermal arsenic(III) in streamwaters of the eastern Sierra Nevada. Environmental Science & Technology, 32(5): 657-662.
World Health Organization, 2006. Managing the quality of drinking-water sources: Section In: O. Schmoll, G. Howard and C. G (Editors), Protecting Groundwater for Health: Managing the Quality of Drinking-water. IWA Publishing, London, pp. 152.
Xu, Y., Schoonen, M.A.A., Nordstrom, D.K., Cunningham, K.M. and Ball, J.W., 2000. Sulfur geochemistry of hydrothermal waters in Yellowstone National Park, Wyoming, USA. II. Formation and decomposition of thiosulfate and polythionate in Cinder Pool. Journal of Volcanology and Geothermal Research, 97(1-4): 407-423.
Yamamura, S. and Amachi, S., 2014. Microbiology of inorganic arsenic: From metabolism to bioremediation. Journal of Bioscience and Bioengineering, 118(1): 1-9.
Zargar, K., Conrad, A., Bernick, D.L., Lowe, T.M., Stolc, V., Hoeft, S., Oremland, R.S., Stolz, J. and Saltikov, C.W., 2012. ArxA, a new clade of arsenite oxidase within the DMSO reductase family of molybdenum oxidoreductases. Environmental Microbiology, 14(7): 1635-1645.
Zhou, E.-M., Xian, W.-D., Mefferd, C.C., Thomas, S.C., Adegboruwa, A.L., Williams, N., Murugapiran, S.K., Dodsworth, J.A., Ganji, R., Li, M.-M., Ding, Y.-P., Liu, L., Woyke, T., Li, W.-J. and Hedlund, B.P., 2018. Thermus sediminis sp. nov., a thiosulfate-oxidizing and arsenate-reducing organism isolated from Little Hot Creek in the Long Valley Caldera, California. Extremophiles, 22(6): 983-991.
Zhu, Y.-G., Yoshinaga, M., Zhao, F.-J. and Rosen, B.P., 2014. Earth Abides Arsenic Biotransformations. Annual Review of Earth and Planetary Sciences, 42: 443-467.